Reviewed Preprint
v1 • November 5, 2025
Not revised

Reviewed Preprint
v2 • May 18, 2026
Revised by authors

For correspondence:
roland@ncnp.go.jp
seki@ncnp.go.jp

Competing interests: No competing interests declared

Funding: See page 32

Reviewing editor: Juan Alvaro Gallego, Champalimaud Foundation, Portugal

Multi-timescale neural adaptation underlying long-term musculoskeletal reorganization

Roland Philipp[1,2], Yuki Hara[3], Naohito Ohta[1,2], Naoki Uchida[1,2], Tomomichi Oya[1,4], Tetsuro Funato[2], Kazuhiko Seki[1]

[1]National Center of Neurology and Psychiatry, Department of Neurophysiology, Tokyo, Japan • [2]University of Electro-Communications, Graduate School of Informatics and Engineering, Dept. of Mechanical and Intelligent Systems Engineering, Tokyo, Japan • [3]National Center of Neurology and Psychiatry, Department of Orthopaedic Surgery, Tokyo, Japan • [4]Western Institute for Neuroscience, University of Western Ontario, London, Canada

eLife Assessment

This **important** study investigates how the nervous system adapts to changes in the mechanics of the body, which are altered through a tendon transfer surgery affecting finger extensor and flexor muscles. By measuring task performance, joint kinematics, and muscle activity for several weeks post surgery, the authors provide **convincing** evidence that monkeys undergo a two-phase adaptation process. First, they adopt a maladaptive strategy to overcome the functional challenges imposed by the surgery, and then revert to a strategy that uses the same patterns of muscle coactivation observed pre-tendon transfer.

https://doi.org/10.7554/eLife.108684.2.sa3

Abstract

The central nervous system (CNS) can effectively control body movements despite environmental changes. While much is known about adaptation to external environmental changes, less is known about responses to internal bodily changes. This study investigates how the CNS adapts to long-term alterations in the musculoskeletal system using a tendon transfer model in non-human primates. We surgically relocated finger flexor and extensor muscles to examine how the CNS adapts its strategy for finger movement control by measuring muscle activities during grasping tasks. Two months post-surgery, the monkeys demonstrated significant recovery of grasping function despite the initial disruption. Our findings suggest a two-phase CNS adaptation process: an initial phase enabling function with the transferred muscles, followed by a later phase abandoning this enabled function and restoring a control strategy that, while potentially less conflicted than the maladaptive state, resembled the original pattern, possibly representing a 'good enough' solution. These results highlight a multi-phase CNS adaptation process with distinct time constants in response to sudden bodily changes, offering potential insights into understanding and treating movement disorders.

Significance statement

After major changes to the body's mechanics, the nervous system adapts using strategies on multiple timescales. Our primate tendon transfer study shows that core muscle synergy groupings remain stable, reflecting a default to modular control. However, the activation of these synergies changes dramatically; an initial, rapid 'swap' of their timing proves to be **maladaptive**, impairing motor function. This conflict is only resolved through the gradual development of **slower,**

compensatory strategies over several weeks. This process highlights the fundamental tension the CNS faces when its reliance on stable motor modules conflicts with the need for flexible control, offering insights into neural plasticity and staged rehabilitation.

Introduction

The central nervous system (CNS) continuously adapts bodily functions in response to both external and internal challenges. Experimental models based on external perturbations, such as altered gravitational fields or distorted sensory feedback, have illuminated mechanisms of sensorimotor adaptation (Sugita, 1996; Davidson and Wolpert, 2003; Luauté et al., 2009; Fleury et al., 2019). Because the changes in the external environment can be controlled by the experimental design, these models provide an opportunity to assess how the CNS adapts to them. However, the transient and predictable nature of these changes may not fully capture the demands posed by internal, long-lasting, and unpredictable alterations to the body's internal environment

In contrast, the internal changes such as developmental growth (Power and Schlaggar, 2017), fatigue (Green, 1997), postural sway (Zemková, 2022), and sensory disorientation (Schärli et al., 2024) impose distinct challenges. Because identifying the source, extent, and time-constant of changes in the internal environment is usually difficult, assessing the corresponding CNS adaptation is also challenging. Particularly, structural alterations to the musculoskeletal system, whether due to injury, disease, or surgery, fundamentally change the body's biomechanics and sensorimotor associations, but the quantification of these changes is usually difficult. Accordingly, the way CNS remaps its motor control strategies corresponding to the changes is not yet well understood (Walker et al., 2004), although understanding such adaptations is crucial for elucidating the pathophysiology of motor impairments observed in chronic musculoskeletal conditions such as osteoarthritis, a degenerative joint disease, (Hunter and Eckstein, 2009) and muscular dystrophy, which involves progressive muscle weakness, (Mercuri and Muntoni, 2013).

To address this question, in this study, we employed a tendon transfer (TT) surgery model (Sperry, 1940), which introduces a controlled, sustained change to the musculoskeletal structure. TT surgery is a clinically well-established procedure (Gardenier et al., 2020) that surgically re-attaches the tendon of a specific muscle to that of a surrounding one. This procedure relocates a specific muscle, so that its contraction generates a new mechanical action and, consequently, novel somatosensory feedback. Because the internal change is controlled by the experimenter, the TT model provides a powerful platform to investigate how the CNS adapts to a new internal state. Another unique feature of TT model is that it places permanent changes of the internal environment while leaving the CNS anatomically intact. Unlike CNS lesion models (Hoffmann et al., 2009), where the injury itself disrupts neural circuits and thereby complicates the assessment of adaptive capacity of the CNS, TT offers a distinct advantage: it allows investigation of CNS-driven adaptation without the confounding effects of direct neural damage. Tendon transfer has been used in various species, with studies suggesting different adaptive capacities, ranging from limited adaptation in adult rodents (Sperry, 1940; Sperry, 1942; Slawinska and Kasicki, 2002; Bowlus et al., 2003) to more substantial adjustments in cats (Yumiya et al., 1979; Loeb, 1999) and primates, including humans (Lee and Seung, 1999; Wester et al., 2018; Gaetz et al., 2023). Therefore, adaptability to TT appears enhanced in primates and humans. Altogether, this approach provides a controlled platform to examine how the CNS adapts to musculoskeletal changes in primates.

According to earlier reports, there are two motor control strategies that could be involved when the CNS needs to face the sensorimotor remapping posed by structural alterations to the musculoskeletal system. First, the CNS may employ modular building blocks such as muscle synergies, coordinated activations of muscle groups that reduce the dimensionality of motor control (d'Avella et al., 2003; Bizzi and Cheung, 2013). Second, skilled behaviors like fine finger movements often require fractionation, the capacity to activate muscles independently. When confronted with structural changes to the musculoskeletal system, does the CNS adapt by

modulating existing synergies, or by shifting toward more fractionated control strategies? Addressing this question requires examining the evolution of neural control strategies over extended periods of recovery to capture both immediate adjustments and long-term learning.

This study aimed to identify long-term adaptive mechanisms of the primate CNS following structural changes to the musculoskeletal system. We investigated whether the CNS adapts by modulating existing muscle synergies or by altering the fractionated control of muscles specifically affected by the surgical alteration. We surgically altered the limb structure by performing crossed tendon transfers of finger extensor and flexor muscle tendons. Using a trained finger-grasping task as our behavioral readout, we examined how the CNS recalibrates muscle activity to regain skilled motor function. Our findings provide new insights into the dynamic reorganization of motor control following structural changes of the body.

Results

In this study, we developed a novel crossed tendon transfer animal model. This involved surgically swapping the tendons of two antagonistic finger muscles in a macaque monkeys' forearm (Fig. 1; A complete list of all muscle abbreviations, their full names, and their assigned synergies for each monkey is provided in Supplementary Table 1). The effectiveness and consistency of the surgery was confirmed by measuring: (i) the distance traveled by muscle fibers and their intramuscular tendons in the transferred muscle (Fig. 2B, C); and (ii) the amount of fingertip displacement (Fig. 2D, E). Both measurements were induced by percutaneous electrical stimulation over the transferred muscles (Fig. 2A). For a detailed description of the results of these measurements see the Methods section. The two monkeys were assigned slightly different tasks, allowing us to examine controlled grasping in Monkey A and a more natural grasp in Monkey B (refer to the Methods section, and Figs. 3 and Fig. 4 for further details). The two monkeys ultimately performed related but distinct grasping tasks, a methodological divergence that provided a valuable opportunity to test the generality of the core adaptive mechanisms. Monkey A performed a controlled grasping task requiring a fine precision grip, designed to study adaptation of fine motor control (Fig. 3). While the same task was initially planned for both animals, Monkey B performed this task inconsistently, frequently varying its grip strategy, and we could not reinforce this monkey to perform in single strategy consistently. Therefore, to ensure reliable task engagement and in accordance with the ethical principle of Reduction and Refinement (the '3Rs'; (Tannenbaum and Bennett, 2015)), the task for Monkey B was modified to a more naturalistic food retrieval grasp that the animal performed consistently (Fig. 4).

Once the monkeys had mastered their respective tasks, we recorded control sessions and then performed the crossed TT. Post-surgery, and once the monkeys had fully recovered and were able to perform the task independently (~3–4 weeks), EMG recordings and behavior were resumed.

Functional Recovery Follows a Biphasic Trajectory

Despite the now reversed roles of the transferred muscles, the monkeys were able to recover their grasping performance within two months, assessed by both the return of key behavioral metrics to pre-surgical levels (Fig. 5A, D) and their consistent ability to perform the task independently (Supplementary Videos S3, S4, S7). However, this recovery was not immediate. The monkeys spent a period of 1-2 weeks in their home cages for recovery, followed by several weeks of assisted task practice. Formal recordings began once the monkeys could perform the task consistently without assistance. The initial post-surgical period was defined by a phase of significant motor impairment, primarily characterized by off-target reaching trajectories (Fig. 5B, E) and prolonged grip formation times (Fig. 5A, D). These off-target reaching movements included inefficient, 'explorative' trajectories in Monkey A and target overshoots in Monkey B (Supplementary Videos S2, S3, S6). This recovery process was quantified across several behavioral and kinematic metrics (Fig. 5). A comparison of pre-TT behavioral variability on the grip formation task (Fig. 5D) revealed that Monkey B was substantially more variable (CV = 81.93%) than Monkey A (CV = 46.62%). This difference in variance was highly statistically significant (Ansari-Bradley test, $p < 0.0001$), confirming a difference in baseline stability between

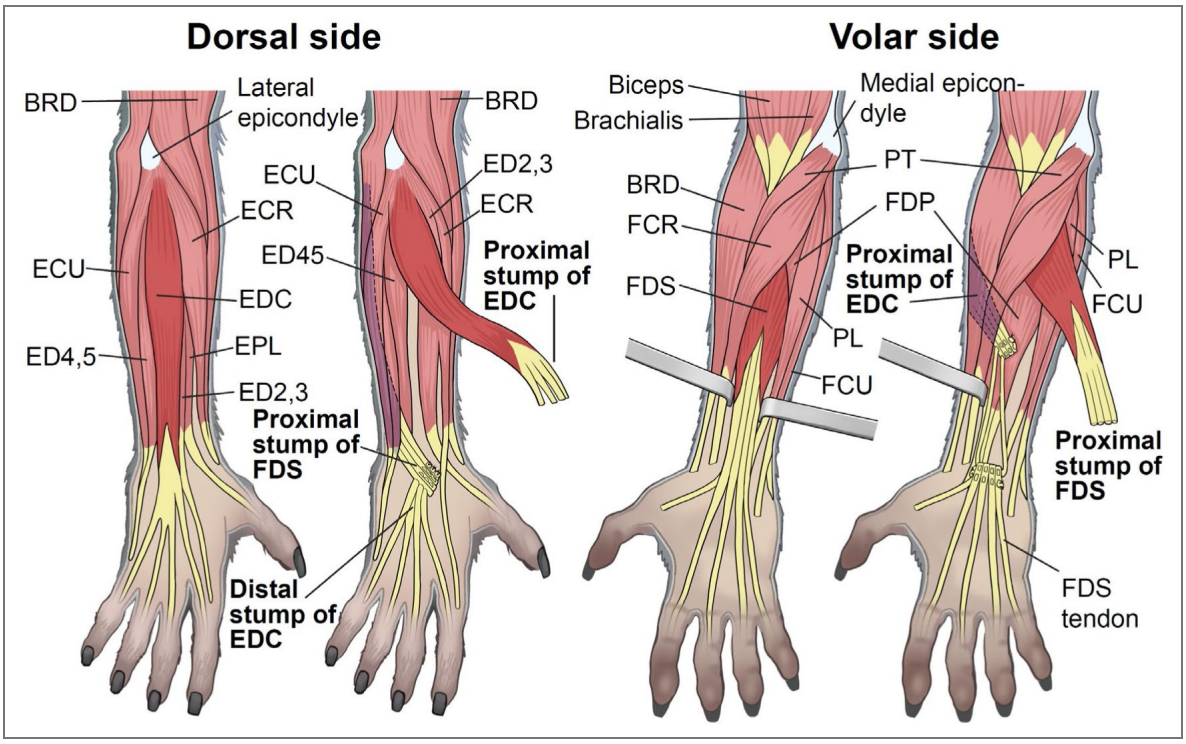

Figure 1. Muscle anatomy of the macaque forearm and the tendon transfer procedure.

A schematic of the primary forearm muscles involved in the study, showing both the dorsal and volar views. The diagram illustrates the surgical crossed tendon transfer of the extensor digitorum communis (EDC) and flexor digitorum superficialis (FDS) tendons. All labeled muscles were implanted with EMG electrodes. Muscle Abbreviations: BRD: brachioradialis, ECR: extensor carpi radialis, ECU: extensor carpi ulnaris, ED2,3: extensor digitorum-2,3, ED4,5: extensor digitorum-4,5, EPL: extensor pollicis longus (not implanted), FCR: flexor carpi radialis, FCU: flexor carpi ulnaris, FDP: flexor digitorum profundus, PL: palmaris longus, PT: pronator teres (not implanted), (The deltoid (DEL) muscle was also implanted in Monkey B but is not shown as it is a shoulder muscle). See also Supplementary Table 1 for a complete list of all muscle abbreviations, their full names, and their assigned synergies.

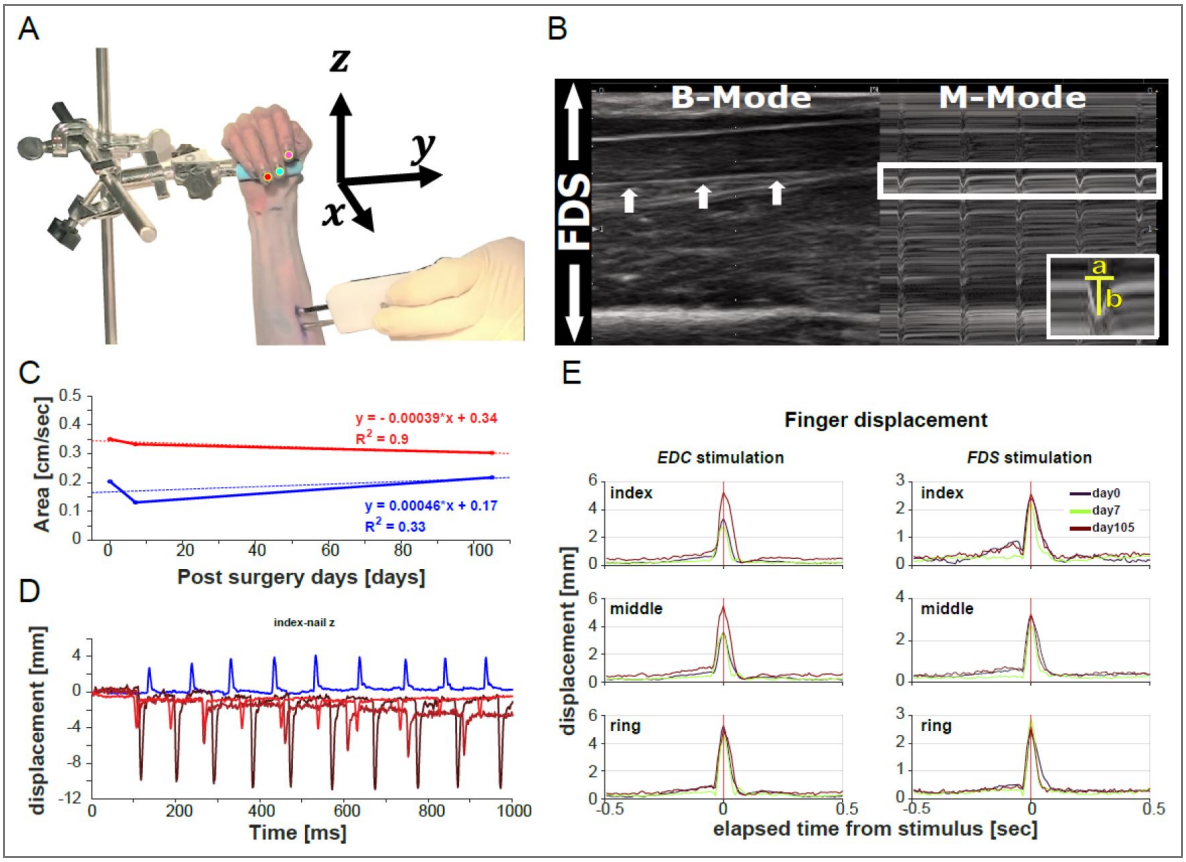

Figure 2. Long term confirmation of tendon surgery effectiveness to alter mechanical properties.

(A) Set-up for the ultrasound measurement and video recordings of the stimulation induced movements of the EDC and FDS tendons. (B) Sonogram of the FDS muscle and its intramuscular tendons. Left side (B-mode, i.e., brightness mode) shows the still image of the monkeys forearm at a given point in time. Right side (M-mode, i.e., motion mode) shows the stagged images of the FDS tendon displacement induced by muscle stimulation (50mA). White arrows demarcate the FDS tendon which was used for the measurement. Grayscale gradations correspond to tissue densities: hyperechoic regions (white) denote denser structures like surface of bones and tendons, while hypoechoic areas (black) signify less dense tissues such as adipose tissue and musculature. Inset demonstrates the area measurement. The area of the displacement waves was measured in the M-mode, representing the strength of muscle contraction. We measured the duration (a, sec) and amplitude (b, cm) of three waves and calculated the average. Area = a*b/2(cm/sec) for days 0, 7 and 105 after tendon transfer. (C) Areas under the wave measured in the M-mode for 3 experimental days (0, 7 and 105 days post-TT) and regression lines in red and blue for FDS and EDC, respectively. R^2>0.5 for FDS. The data suggested that muscle contractions induced by direct electrical stimulation were nearly constant. (D) Markers placed on the index, middle and ring finger nails (A) were used to measure finger displacement in xyz-dimensions. We calculated the sum of the Euclidean distances of each marker from the origin of the 3D coordinate system as a scalar quantity. Observing the movement along the Z-axis, it became reversed post-surgery indicating a reversal from finger flexion to extension due to tendon transfer (D, blue = pre-TT at surgery day; dark brown = post-TT at surgery day; light brown = 1wk post-TT; red = 3wks post-TT). The scalar quantity of the fingers during muscle stimulation did not change much at day 0, 7 and 105 days (E), suggesting that there was no tendon rupture or slackening of the tendons postoperatively (EDC stimulation, left; FDS stimulation, right). Data were collected in monkey A.

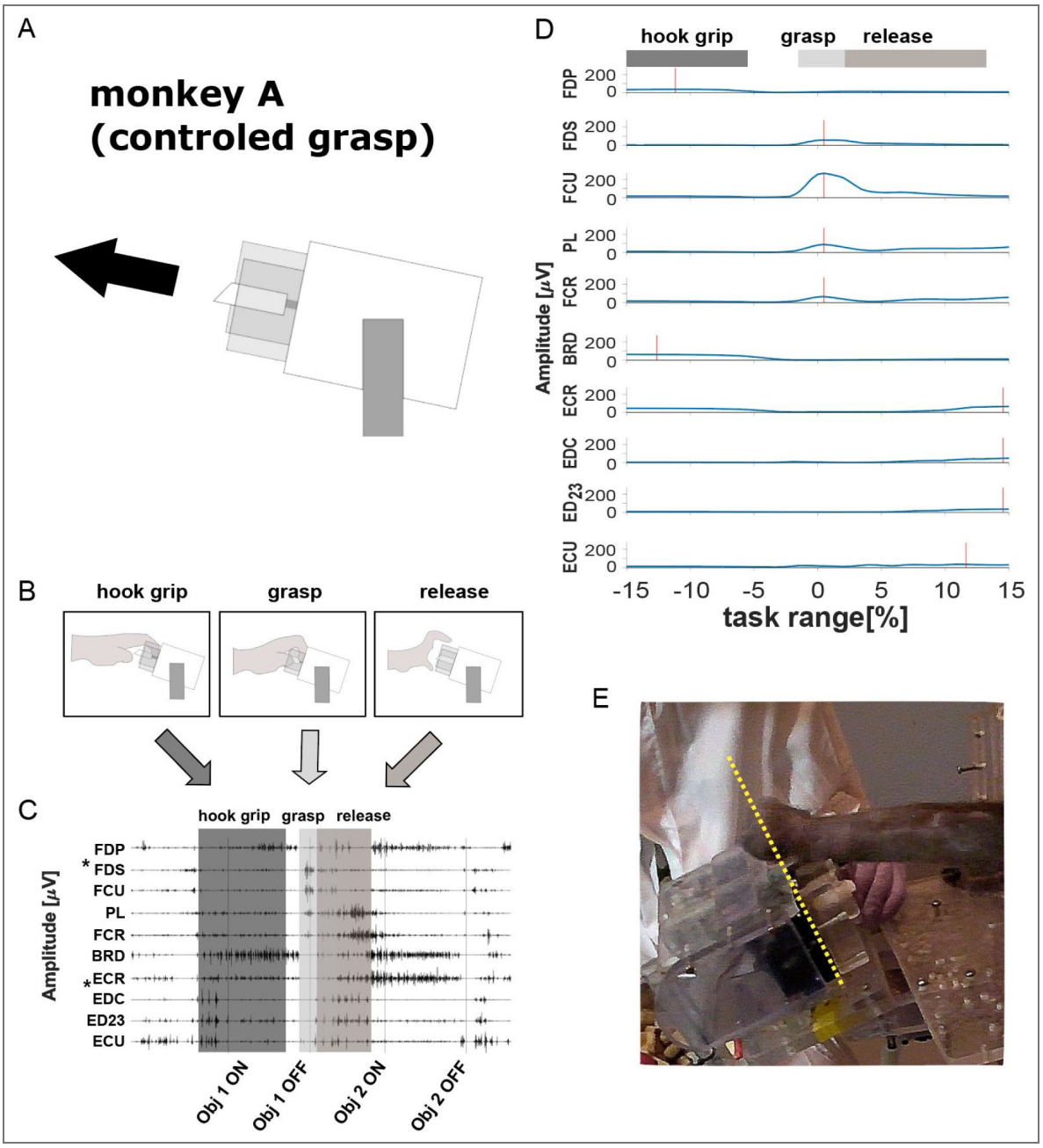

Figure 3. Experimental set-up, task sequence and typical EMG (monkey A).

(A) Schematic of the task object using a rod requiring monkey A to perform a controlled grasp. (B) Schematic of the behavioral sequence (hook → grasp → release). (C) Typical EMG traces of a control session (high-pass filtered) for all recorded muscles. Gray boxes represent the task sequence. Obj 1 ON: start of the hold period of object 1. Obj 1 OFF: end of the hold period of object 1, i.e., object release. Obj 2 ON: start of the hold period of object 2. Obj 2 OFF: end of the hold period of object 2, i.e., object release. Tendons of the muscles marked with * were cross-transferred. (D) Rectified and smoothed EMG for all recorded muscles (average for one recording session; amplitude [μV] over task sequence [%]). Horizontal bars illustrate the corresponding behavioral periods; red vertical lines indicate peak amplitude for each muscle). (E) The time the monkey spent on the left side of the yellow dotted line while moving from object 1 to object 2 was measured and used to quantify the maladaptive behavior.

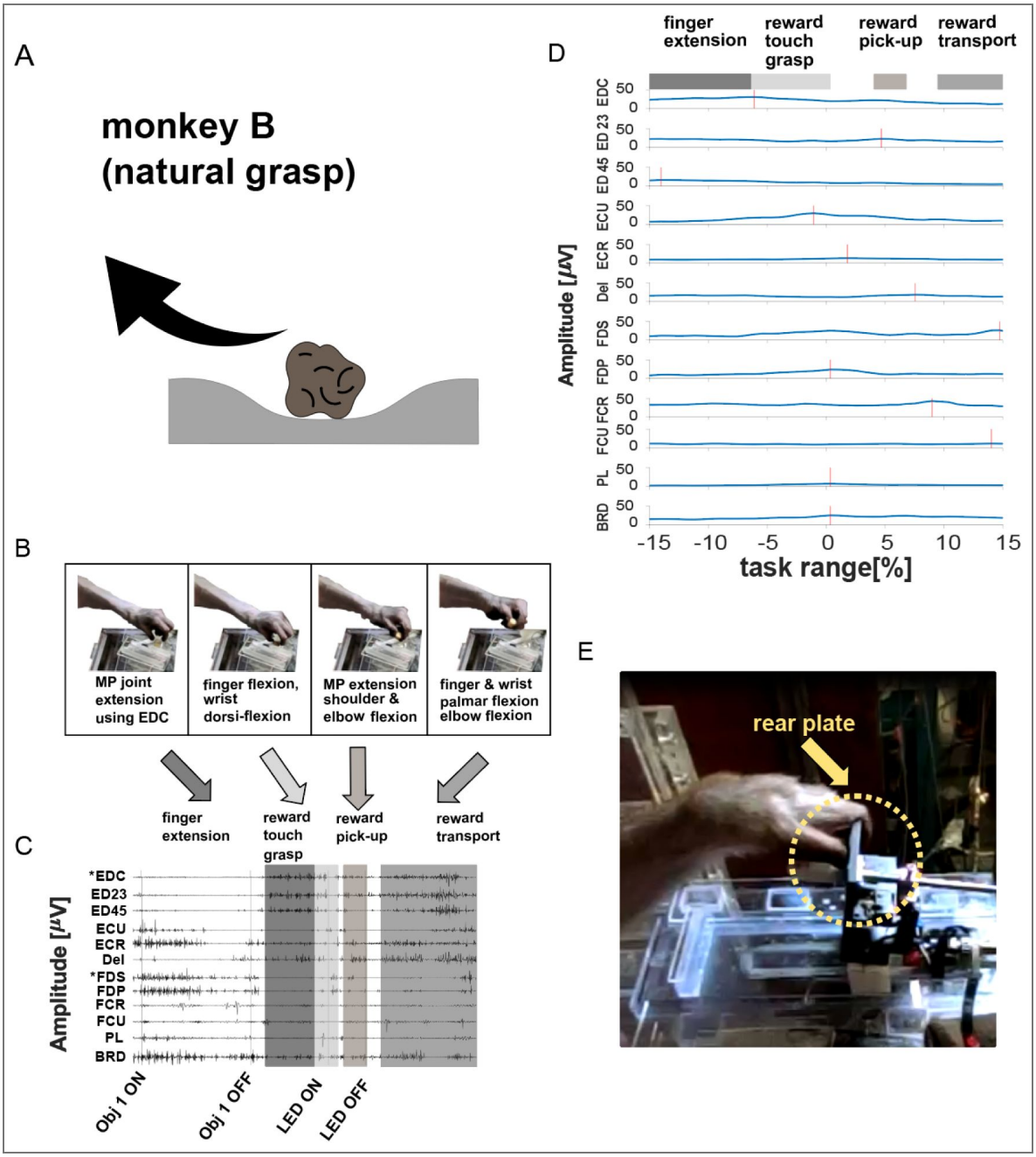

Figure 4. Experimental set-up, task sequence and typical EMG (monkey B).

(A) Schematic of the task requiring monkey B to pick up food from a groove allowing for a more natural grasp. (B) Schematic of the task sequence (picking up food). (C) Typical EMG traces of a control session (high-pass filtered) for all recorded muscles. Gray boxes represent the task. Obj 1 ON: start of the hold period of object 1. Obj 1 OFF: end of object 1's hold period, i.e. object release. LED ON: approximate start of the food touch. LED OFF: approximate time of food retrieval. Tendons of the muscles marked with * were cross-transferred. (D) rectified and smoothed EMG for all recorded muscles (average for one recording session; amplitude [μV] over task sequence [%]). Horizontal bars illustrate the corresponding behavioral periods, red vertical lines indicate peak amplitude for each muscle). (E) Example for maladaptive behavior in monkey B. The time the monkey spent in contact with or behind the object plate was measured and used to quantify the maladaptive behavior.

the subjects likely due to the less constrained nature of Monkey B's task. Post-surgery, variability in grip formation time initially increased dramatically for Monkey A (Early Phase CV = 132.98%), while remaining high for Monkey B (Early Phase CV = 76.46%). In the late phase, Monkey A's variability stabilized slightly above baseline (Late Phase CV = 54.79%), whereas Monkey B's variability increased further, exceeding its pre-TT level (Late Phase CV = 96.59%), suggesting persistent inconsistency in grasp timing for this animal. Variability patterns differed for the other metrics: Monkey A's pull time variability decreased below baseline in the mid and late phases (Pre CV = 64.97%, Mid CV = 41.30%, Late CV = 43.01%), indicating a refinement of this action, while Monkey B's grasp aperture variability remained consistently low throughout recovery (Pre CV = 26.37%, Early CV = 23.80%, Mid CV = 19.78%, Late CV = 19.35%). The initial post-surgical period was defined by motor performance that we classify as maladaptive due to the persistence of inefficient, off-target reaching and prolonged movement durations. First, task-related grip formation times were significantly longer immediately post-TT (Monkey A: 197.7 ±92.2 vs. 660.6 ±221 ms, p = 0.014; Monkey B: 169.7 ±14 vs. 316.3 ±31.9 ms, p = 0.016), taking approximately 40 days for Monkey A and 48 days for Monkey B to return to and stabilize at pre-surgical levels (Fig. 5A, D). Second, the duration of off-target reaching was substantially elevated, stabilizing approximately after 70 days in Monkey A and 55 days in Monkey B (Fig. 5B, E). Following this phase, motor performance showed a gradual recovery in efficiency (Fig. 5C) and kinematics (Fig. 5F). Ultimately, overcoming these initial maladaptive behaviors through the gradual refinement of motor performance led to the stabilization of grasping by the end of the experimental period.

A two-phase adaptation is observed in the EMG activity of individual muscles

Initially, we investigated whether EMG activity exhibited any changes post-TT. Given that we interchanged the tendons of an antagonistic muscle pair, functionally rendering the FDS an extensor and the EDC a flexor (as confirmed mechanically, Fig. 2), a biomechanically sound adaptation would be to use the former finger extensor (EDC) for finger flexion, and the former finger flexor (FDS) for finger extension during a grasping task. We therefore analyzed EMG activity from both transferred and non-transferred muscles to determine if these expected functional changes occurred. Figure 6 shows a comparison of EMG activity profiles for the two transferred muscles, EDC and FDS, in Monkey A (Fig. 6A–D). Prior to surgery, the control showed distinct and contrasting EMG profiles in both muscles. For instance, peak activity in EDC (▾) occurred long after completion of the grasping action (indicated by vertical dashed lines at 0% task range) at 15% task time (Fig. 6A), coinciding with the animal pre-shaping its hand to prepare for the subsequent grasp. Whereas peak activity in FDS (▽) was observed immediately after completion of the grasping action (0.49%; Fig. 6C). The question we posed was whether the post-surgery activity of EDC resembled its original profile (without adaptation to surgery) or the activity of FDS (the anticipated profile following surgical adaptation), and vice versa. Our findings suggested that EMG activity patterns largely shifted in a manner consistent with the new mechanical function imposed by the transfer. Early after TT, peak activity of EDC occurred at −0.58% task time (Fig. 6B; days 29 [red line] and 64 [orange]), which aligns with peak activity of FDS prior to TT (Fig. 6C; black line). Also, for FDS, peak activity occurred at 11% task time (Fig. 6D; ▾), which aligned with peak activity of EDC (Fig. 6A).

This was corroborated by the results in Monkey B (Fig. 6, panels K-M). Although the EMG patterns of both muscles varied significantly as the two monkeys performed different types of grasping actions, we found that the EMG of EDC peaked at −6.12% before (Fig. 6K; ▾) and 0.35% and 1.05% after TT (Fig. 6L; ▽, days 22 and 36, respectively), closely matching the timing for FDS control data (Fig. 6M). The corresponding analysis for FDS could not be performed in Monkey B, since the EMG signal of FDS was lost early after TT (see Methods for details). We were able to extend our recordings to 122- and 64-days post-TT for monkeys A and B, respectively. This allowed us to examine whether the adaptations observed in the early period were consistent throughout the experimental period. These additional days (Fig. 6B, D; 69 [cyan], 79 [blue], and 99 [black]

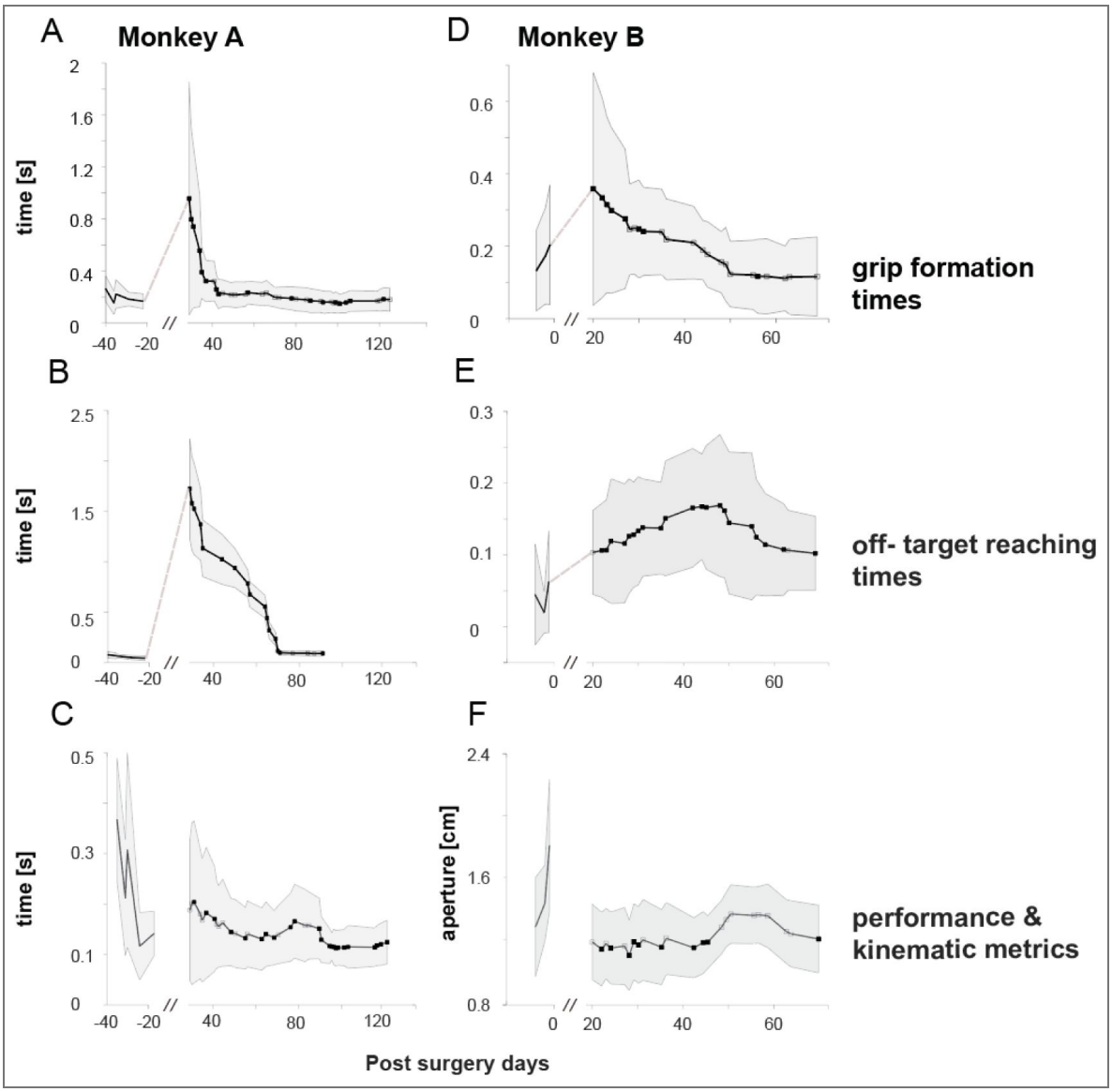

Figure 5. Behavioral and kinematic metrics of motor recovery.

(A, D) Grip formation times (mean ± SD; n = 20 trials) for Monkey A (A) and Monkey B (D). (B, E) Duration of off-target reaching movements (mean ± SD; n = 10 trials) for Monkey A (B) and Monkey B (E). (C) Pull time duration for Monkey A. (F) Grasp aperture size for Monkey B. Filled squares indicate significant difference from pre-TT baseline ($p < 0.05$, two-sample t-test). All data are plotted over days relative to tendon transfer (TT).

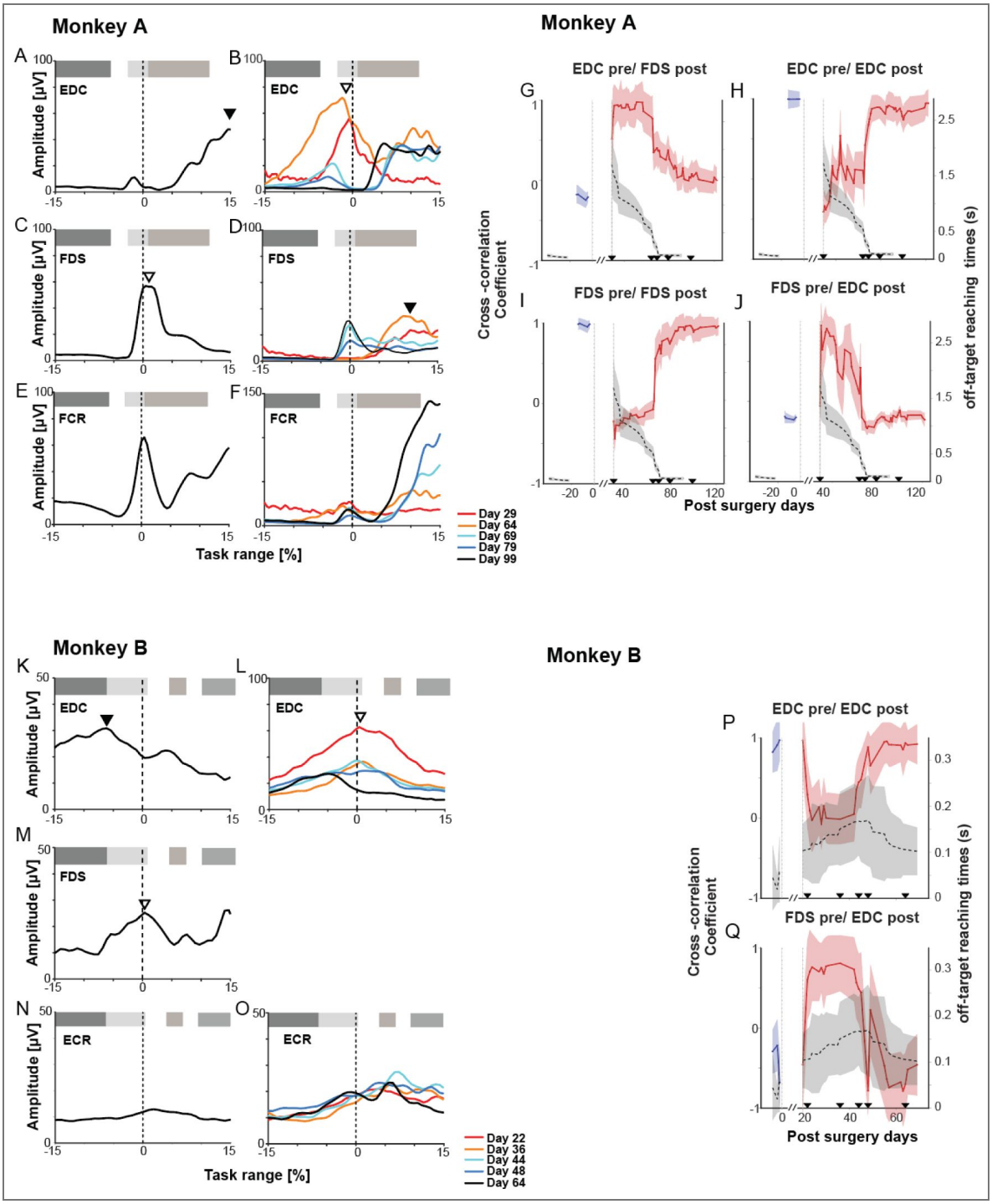

Figure 6. Temporal EMG profiles and cross-correlation analysis.

Temporal EMG profiles for Monkey A (left, A-J) and Monkey B (right, K-Q). (A-F, K-O) Average EMG activity profiles aligned to task events (0%; object release for A, food touch for B). Shaded envelopes represent standard deviations. Triangles indicate peak activity during extension (▾) or flexion (▽). Colored traces denote post-surgery landmark days. (A-D, K-M) Comparison of transferred muscles. Note the temporal shift in the post-surgery profile (B, L) relative to the pre-TT baseline (dashed lines). (E-F, N-O) Profiles of non-transferred muscles. (G-J, P-Q) Zero-lag cross-correlation coefficients between post-surgery EMG profiles and the pre-TT baseline profiles plotted over time. (H, I, P) Correlation coefficients calculated against the muscle's *own* pre-TT baseline. (G, J, Q) Correlation coefficients calculated against the *antagonist's* pre-TT baseline (e.g., Post-EDC vs. Pre-FDS). Black dashed lines on the right y-axis indicate behavioral error metrics (Off-target reaching time for Monkey A; Contact duration for Monkey B; gray shading represents SD). The // represents the recovery period.

post-TT; see Fig. S1 for recordings from all days) showed that the EMG activity profiles for both muscles unexpectedly returned to their pre-TT state. For example, as already described, the EMG signal of EDC at days 29 and 64 shared the characteristics of FDS, but by the following day (only 5 days later, day 69 [light blue] post-TT) already exhibited pre-TT characteristics of EDC, continuing as such until the end of the recording period (day 79 [blue] and 99 [black]). This was confirmed for the EDC muscle of Monkey B (Fig. 6K, L; Fig. S1U-AO for recordings from all days).

To relate these neural changes to functional recovery, we overlaid the behavioral error metric (off-target reaching time; gray dashed lines) onto the cross-correlation plots (Fig. 6G–J). Figure 6H (red line) illustrates cross-correlation coefficients between the EDC EMG profile post-TT (EDC-post) and the original EDC control data (EDC-pre) in Monkey A. Figure 6I shows coefficients for EDC-post and FDS-pre correlations in the same monkey. The coefficient corresponding to the original profile decreased to between −0.3 and 0.2 over approximately 65 days (Fig. 6H). In contrast, the coefficient corresponding to the expected EMG profile exhibited an inverse pattern, with low coefficients pre-TT and a high coefficient (of 0.9) post-TT (Fig. 6J). Cross-correlation analysis for FDS (Fig. 6G, I) revealed a similar pattern. Cross-correlation coefficients for FDS-pre- vs. FDS-post analysis declined from 1 to negative values, only to rebound to their original values within a month (day 79; Fig. 6G). This outcome aligns with our previous observations (Fig. 6B, D), and were corroborated by the results from Monkey B (Fig. 6K-Q). Here, cross-correlation coefficients dropped from +0.95 to +0.1 for EDC-pre vs. EDC-post comparison, and increased from −0.5 to 0.9 for the FDS-pre vs. EDC-post comparison (Fig. 6P, Q). After 42 days post-TT, cross-correlation coefficients started to gradually increase or decrease to +0.9 and −0.7, respectively. This indicates that the anticipated initial changes in EMG activity profiles are not permanent. Instead, they revert to their original patterns two months post-TT. A supplementary analysis of the time lag at peak correlation (Supplementary Figure S1) confirmed that the optimal lag for individual muscles also fluctuated significantly during the early adaptive phase before stabilizing, reflecting the process of temporal re-coordination of individual muscle commands.

Interestingly, changes in EMG pattern were not isolated to the transferred muscles; non-transferred muscles exhibited a variety of complex adaptations (Figs. 6, S2-S4). A comprehensive overview of the average EMG profiles for all recorded muscles across all recording sessions and landmark days is provided in Supplementary Figures S2 (Monkey A) and S3 (Monkey B), respectively. As shown in these figures, many agonists adapted in concert with their transferred synergist, following the same two-phase “swap-and-revert” pattern seen in Figure 6. In Monkey A, these included extensors ED23 and ECU, while in Monkey B, they included ED23, ED45, and ECU (see Fig. S2 for details). In contrast, other muscles showed patterns that were incompatible with a simple swap. For example, the non-transferred flexor carpi radialis (FCR) in Monkey A showed a distinct adaptive profile characterized by a drastic initial decrease in one activity peak and a consistent increase in a later peak (Fig. 6E, F). A similar incompatible pattern was seen in palmaris longus (PL) (Fig. S1H, I, R, S). Finally, some muscles, like the extensor carpi radialis (ECR) in Monkey B, remained relatively stable post-surgery (Fig. 6N, O). These diverse patterns in non-transferred muscles do not necessarily contradict a modular control strategy (d’Avella et al., 2003; Bizzi and Cheung, 2013); rather, they likely reflect the fact that different muscles are primary members of different synergies (i.e., they possess the highest weightings within specific modules; e.g., FCR and PL in Synergy C), each undergoing its own task-specific adaptation.

Adaptation occurs through modulating the activation of stable muscle synergies

To determine whether the CNS adapted by fractionating muscle control or modulating existing modules, we extracted muscle synergies using non-negative matrix factorization (NMF) (Lee and Seung, 1999). Four synergies accounted for >80% (Cheung et al., 2012) of the variance in both monkeys (see Supplementary Figure S5 for VAF plots; >85% for both monkeys; the results of the original and shuffled data sets are shown. See also the synergy weights [*W*] and activation profiles

[*C*] for both monkeys and all synergies in figs. S6 and S7, respectively). We first focused on the two primary synergies responsible for the main task axis: the finger flexor synergy (Synergy A) and the finger extensor synergy (Synergy B) (Fig. 7).

We first analyzed whether the spatial structure of these primary synergies changed. To distinguish genuine adaptation from natural variability, we established a baseline by calculating the cosine similarity of spatial synergy weights (*W*) across all pre-surgery days (Fig. 7I, J, blue traces). This revealed remarkably high stability (>0.99). Post-surgery, the core structure remained conserved. The cosine distance between pre- and post-surgery weights for the same synergy pairs was low (Monkey A: 0.03 ± 0.03; Monkey B: 0.09 ± 0.11), whereas for different pairs it was high (>0.60). This confirms that the CNS maintained the stable, neurally constrained building blocks of the primary flexor and extensor modules despite the altered biomechanics.

In contrast to the stable spatial structure, the temporal activation profiles of these primary synergies underwent drastic changes. In Monkey A, the flexor Synergy A (originally peaking at +0.97% task time) and extensor Synergy B (originally peaking at 12.62%) swapped their timing profiles shortly after surgery (Fig. 7C, D). Specifically, the extensor synergy shifted to peak during the flexion phase, and vice versa. This "swap" persisted during the early impairment phase before reverting toward the original timing in the late phase. A similar "swap-and-revert" pattern was observed in Monkey B (Fig. 7G, H), where the extensor Synergy B shifted from a pre-surgery peak at −8.75% to a post-surgery peak of +3.5% (matching the flexor phase) before recovering.

To formally quantify the quality of this reversion, we compared the pre-surgery activation profiles with those from the final day of recording. We found that while the temporal shape was highly preserved (Cosine Similarity >0.90), the profiles remained statistically distinct (Permutation Test, $p < 0.0001$; Fig. S8). This confirms that the recovered motor program represents a "good enough" functional approximation rather than a perfect mathematical restoration of the baseline.

We next examined the secondary synergies involved in wrist control and stabilization (Fig. 8). In contrast to the coherent "swap" seen in the primary synergies, these modules exhibited distinct, task-specific adaptations.

In Monkey A, Synergy C (a wrist flexor synergy involving PL and FCR) showed a temporal shift that was incompatible with a simple swap (Fig. 8C). While its spatial weights remained stable (Fig. 8A, I), its activation peak shifted from the post-grasp phase (+1.46%) to the pre-grasp phase, increasing in magnitude over time. This pattern corresponds to the recruitment of wrist flexors to enable the compensatory tenodesis grasp. Synergy D (wrist extensor) underwent a single notable change on day 29 but quickly reverted (Fig. 8D). In Monkey B, Synergy C showed no discernible trend (Fig. 8G), while Synergy D exhibited a complex pattern of immediate change followed by a gradual shift in the late adaptation period (Fig. 8H). Notably, the activation amplitude of Synergy D remained significantly suppressed compared to baseline (Fig. 8H; Fig. S6H). This suppression of the wrist extensor likely reflects the specific biomechanical requirements of the tenodesis strategy employed by Monkey B: relaxing the wrist extensors facilitates the necessary wrist flexion for hand opening. These independent changes in secondary synergies likely served to reinforce the overall functional recovery driven by the primary modules.

Again, the characteristics of these changes in activation profiles of muscle synergies were also quantitatively confirmed by cross-correlation analysis of all four muscle synergies in both monkeys. The coefficients were plotted over the course of experimental days in relation to tendon surgery together with the overlaid behavioral error metric (off-target reaching time; gray dashed lines) (Fig. 9). In this analysis, the activation profile of each synergy was cross-correlated with either the one from synergy A (finger flexor synergy; Fig. 9C, D, G, H) or synergy B (extensor synergy; Fig. 9A, B, E, F) before TT. As previously demonstrated for the FDS and EDC muscles, the temporal activation profiles of muscle synergies A and B (flexor and extensor) displayed a distinct pattern. After cross-correlation with their own control data, both the flexor and extensor synergies showed coefficients of 1 prior to surgery. These became negative for 66 days post-surgery before reverting close to their original values (Fig. 9B, C). However, after cross-correlation with control data of the antagonistic muscle synergy (i.e., extensor for flexor synergy and vice versa, Fig. 9A,

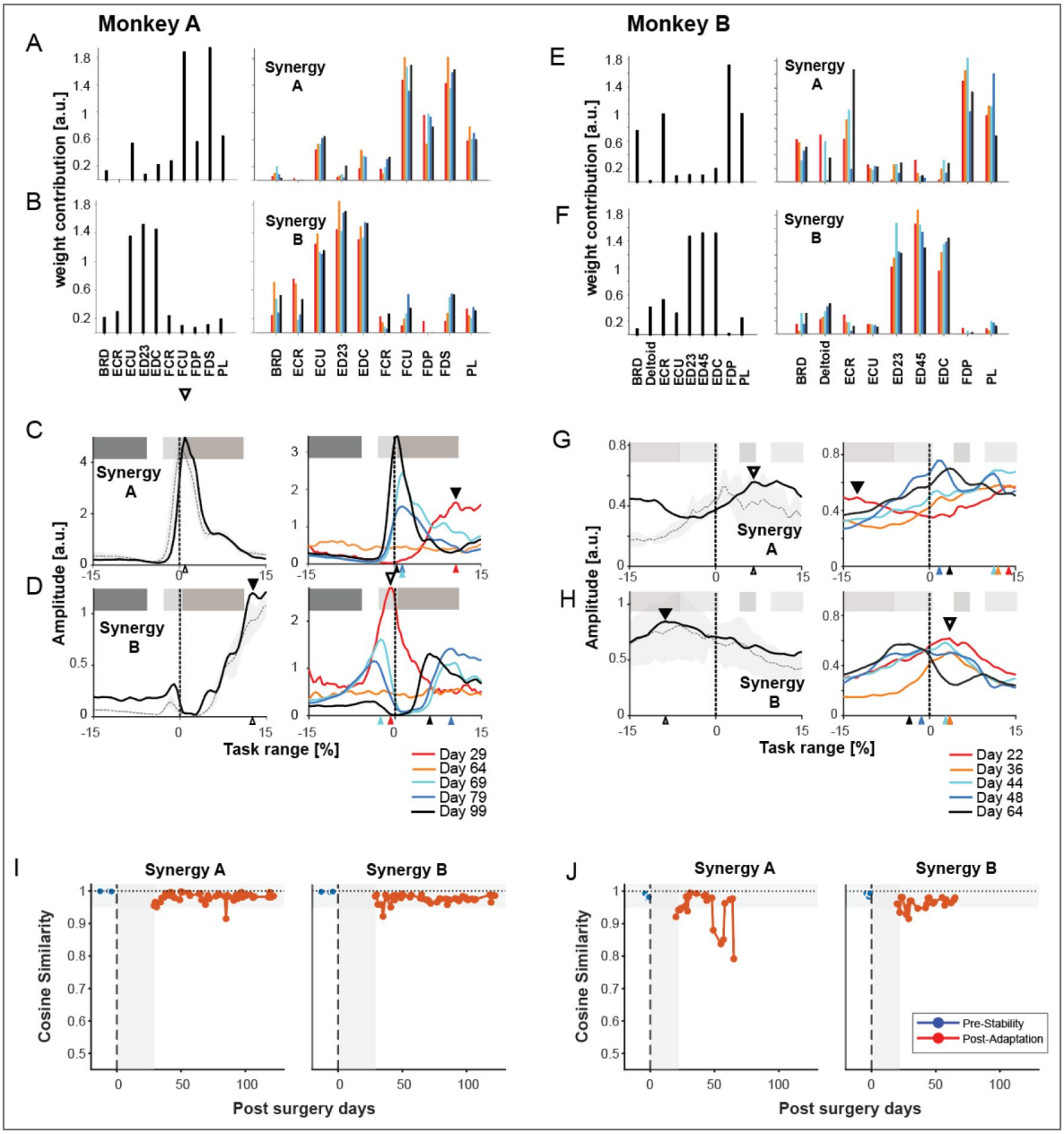

Figure 7. Spatial structure and temporal activation of Primary Synergies.

Analysis of the two primary synergies: Synergy A (Flexor) and Synergy B (Extensor). (A, B, E, F) Spatial synergy weights (*W*) showing the contribution of each muscle to the synergy. Bar plots represent the average weights across all recording days. (C, D, G, H) Temporal activation profiles (*C*) aligned to task events (0%). Dashed lines with shaded tubes indicate the average pre-TT EMG profiles of the key contributing muscles (FDS, EDC, FDP) for visual comparison with the synergy profile. Symbols and alignment are as described in Figure 6. (I, J) Quantification of spatial stability. Cosine similarity of spatial synergy weights (*W*) calculated between individual recording days and the pre-TT average. Blue markers indicate pre-TT control days; Red markers indicate post-TT days. The horizontal gray shaded region (0.95-1.0) denotes the range of high baseline stability.

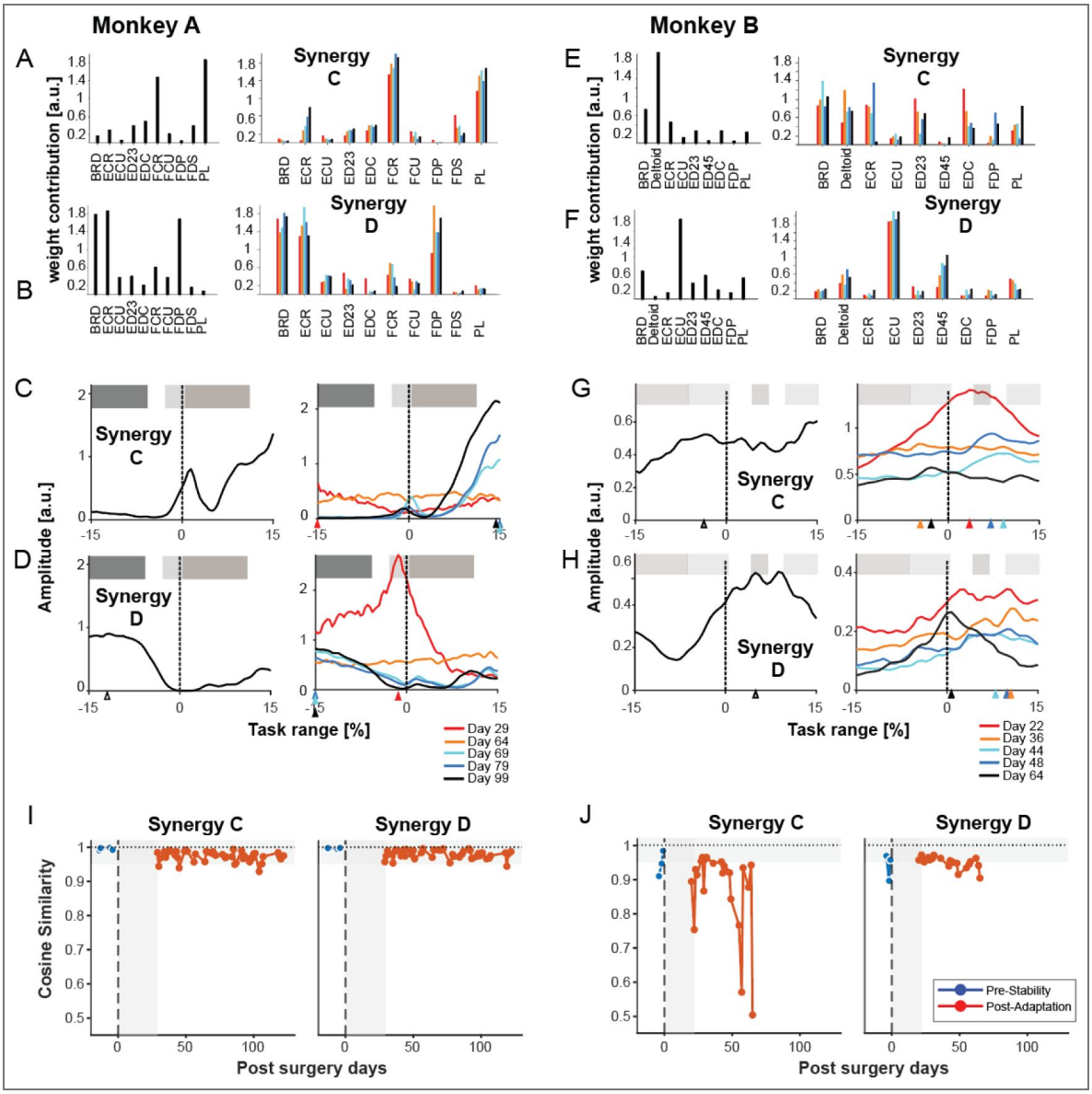

Figure 8. Analysis of Secondary Muscle Synergies.

(A-H) Analysis of Secondary Synergies C (Wrist Flexor) and D (Wrist Extensor). (A, B, E, F) Spatial synergy weights (*W*) showing the contribution of each muscle. (C, D, G, H) Temporal activation profiles (*C*) aligned to task events (0%). Colored traces denote post-surgery landmark days. Layout and symbols are as described in Figure 6. (I, J) Quantification of spatial stability for Synergies C and D. Cosine similarity of spatial weights calculated between individual recording days and the pre-TT average. Blue markers indicate pre-TT control days; Red markers indicate post-TT days. The horizontal gray shaded region (0.95-1.0) denotes the range of high baseline stability.

D), the pattern was reversed. Coefficients started with negative values prior to TT and shifted to positive coefficients near 1 shortly after surgery. In Monkey A, coefficients returned to negative values around day 66 post-TT. In Monkey B, this reversal occurred earlier, around day 48. In short, these results mirror our findings between the transferred muscles (Fig. 6G, J). Furthermore, to determine if low correlations were driven by simple timing mismatches, we analyzed the optimal time lag yielding the maximum cross-correlation (Supplementary Figure S9). A positive lag indicates the post-surgery activity is delayed relative to baseline, while a negative lag indicates it is advanced. This analysis revealed significant fluctuations in timing (switching between delays and advances) during the early and mid-adaptation phases, particularly around the 'switch-back' period, before stabilizing closer to zero lag in the late phase. For synergies C (main contributing muscles: ECR, BRD, DEL) and D (main contributing muscles: ECU), the changes in cross-correlation coefficients over time were markedly different. For synergy C, coefficients begin to steadily increase when cross-correlated with control data of the extensor synergy (synergy B, Fig. 10E), and decrease with the flexor synergy (synergy A, Fig. 10G). This suggests an increasing contribution to finger extension. In contrast, synergy D does not exhibit any specific pattern following TT.

In Monkey B, this cross-correlation analysis revealed a more varied, or differential, pattern of adaptation across the four synergies (Figs. 9 and 10). The primary extensor, Synergy B, mirrored the results in Monkey A, showing a clear swap-and-revert pattern (Fig. 9F, H). In contrast, Synergy A did not show a clear reversal; its correlation coefficients gradually converged towards zero, likely due to the absence of the FDS EMG signal in the analysis (Fig. 9E, G). The secondary synergies, Synergy C and D, showed no discernible trend (Fig. 10E-H).

In summary, both monkeys exhibited a distinct two-phase adaptation following TT. We define the 'early phase' as the period from initial post-surgical recovery up to the reversal of the swapped activation patterns (approximately days 20/29 to ~65 post-TT, see Fig. 9), characterized by the transferred muscles/synergies adopting antagonistic temporal profiles. We also identify a 'mid-adaptation' phase covering the transitional period around the 'switch-back' event, characterized by high variability. The 'late phase' encompasses the period following this switch-back (after ~day 66 post-TT), where original activation timings were largely restored. While this 'reversion' towards original activation timings in the late phase marked the abandonment of the initial maladaptive strategy, behavioral recovery involved more than just restoring original patterns. Concurrent with this neural shift in the primary synergies, a distinct compensatory strategy began to emerge, utilizing secondary synergies and biomechanical coupling to achieve functional hand opening, as detailed below.

The Early Adaptation Phase is Characterized by a Maladaptive Neural and Behavioral Profile

The early adaptation phase was defined by a distinct neural strategy that correlated with significant behavioral deficits. First, the period dominated by off-target reaching movements and prolonged grip times (Fig. 5B, E) was precisely when the swapped activation of Synergy A and B was most prominent (Fig. 9; see behavioral overlay). This temporal link provides strong evidence that this initial 'swap' strategy was, in fact, maladaptive, as the flawed neural control directly underpinned the impairments in movement efficiency and precision.

Second, we found that the net activity of muscles representing certain muscle synergies (aggregated average EMG; aaEMG) showed distinct, synergy-specific changes over time (Fig. 11). A key feature was the evolution of the activity of finger extensor synergy (Synergy B), which appeared to undergo a neuromuscular 'arms race', a rapid escalation of antagonistic co-activation, in both animals, albeit on different timescales (Fig. 11B, J). In Monkey A, which struggled for a longer period to regain behavioral proficiency according to our subjective evaluation, our recordings now captured this process unfolding: we observed a steady and significant increase in Synergy B's aaEMG post-TT until day 64 ($p < 0.0001$) before the strategy changed (Fig. 11B, F). In contrast, Monkey B, which adapted its behavior more rapidly according to our subjective evaluation, showed a different profile; its Synergy B activity peaked with a significant surge early

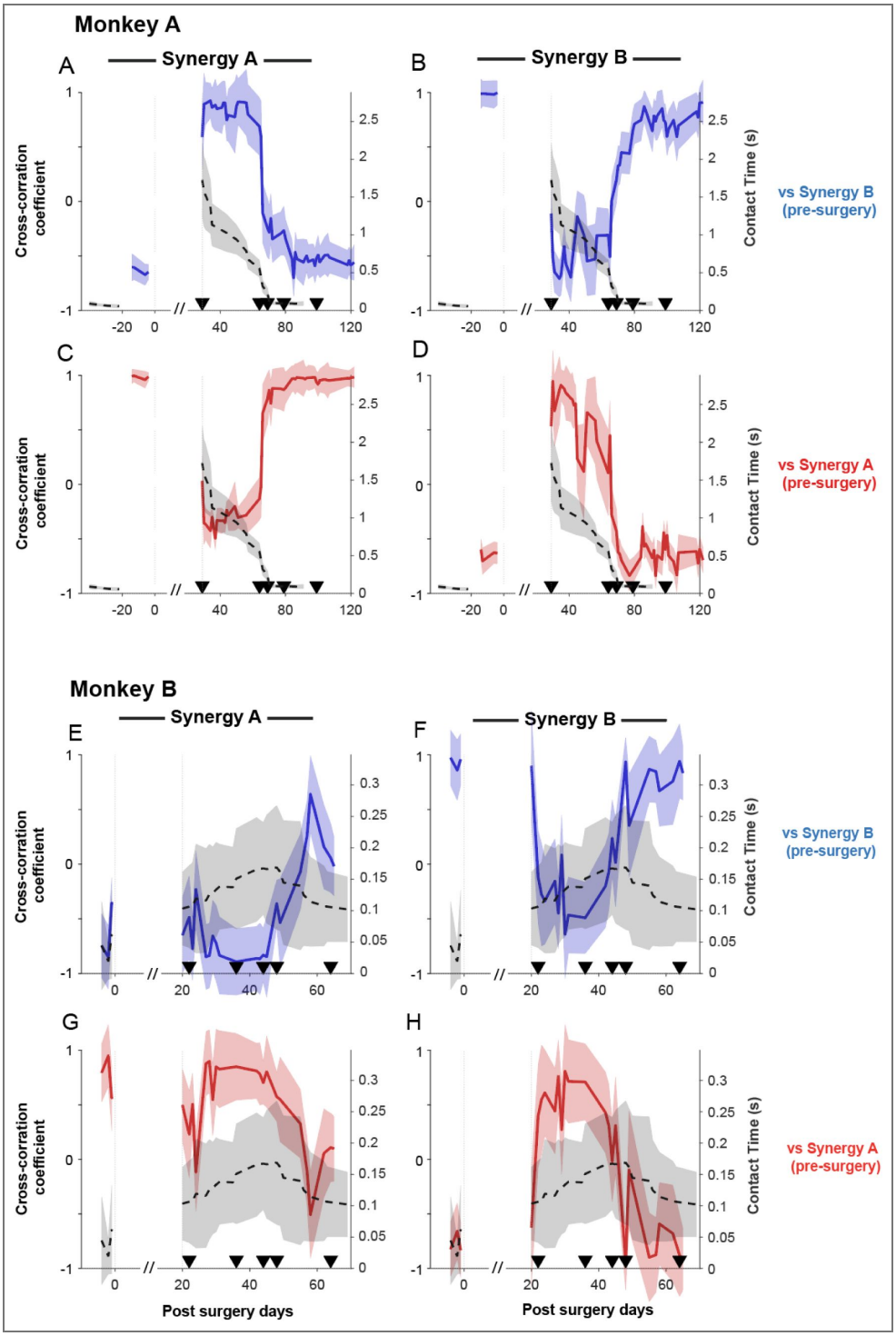

Figure 9. Cross-correlation analysis of Primary Synergy activation.

Zero-lag cross-correlation coefficients plotted over post-surgery days for Monkey A (A-D) and Monkey B (E-H). Activation patterns of the Primary Flexor (Synergy A) and Primary Extensor (Synergy B) were cross-correlated with pre-TT baseline profiles. (Top Row: A, B, E, F) Correlations calculated against the pre-TT *Extensor* Synergy (Synergy B, blue traces). (Bottom Row: C, D, G, H) Correlations calculated against the pre-TT *Flexor* Synergy (Synergy A, red traces). (C, G) Correlation of Synergy A with its own pre-TT baseline. (B, F) Correlation of Synergy B with its own pre-TT baseline. (A, E, D, H) Cross-correlations between antagonistic synergies (e.g., A is Synergy A vs. Pre-Synergy B). Black dashed lines on the right y-axis indicate behavioral error metrics (gray shading represents SD). The // represents the recovery period. Triangles indicate landmark days.

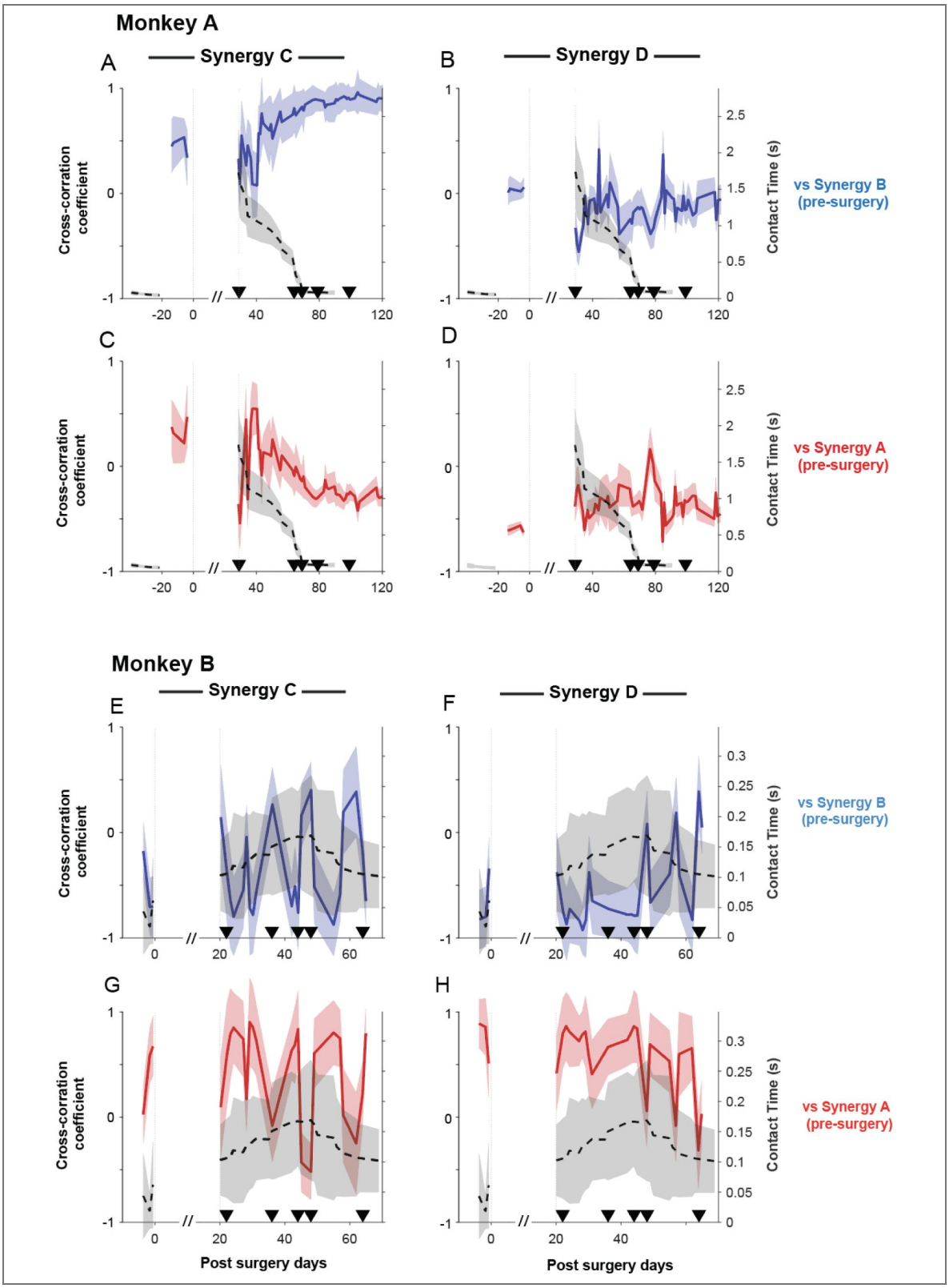

Figure 10. Cross-correlation analysis of Secondary Synergy activation.

Zero-lag cross-correlation coefficients for the secondary synergies (C and D) plotted over post-surgery days for Monkey A (A-D) and Monkey B (E-H). Activation patterns were cross-correlated with the pre-TT profiles of the Primary Synergies to assess changing affiliations. (Top Row: A, B, E, F) Correlations calculated against the pre-TT *Extensor* Synergy (Synergy B, blue traces). (Bottom Row: C, D, G, H) Correlations calculated against the pre-TT *Flexor* Synergy (Synergy A, red traces). (Left Columns: A, C, E, G) Synergy C correlations. (Right Columns: B, D, F, H) Synergy D correlations. Black dashed lines on the right y-axis indicate behavioral error metrics.

in the recording period (day 22: $p < 0.0001$) and subsequently declined toward and below baseline (day 64: $p < 0.001$) (Fig. 11J, N). This suggests the initial, rapid escalation of the 'arms race' in this animal had already occurred and peaked prior to our first post-operative recording session. Therefore, the apparent discrepancy in the evolution of Synergy B is likely not a fundamental difference in strategy, but rather a reflection of the different observational windows and overall adaptation rates of the two animals.

For the finger flexor synergy (Synergy A), Monkey A showed a general decrease in activity ($p = 0.0004$ at day 79; Fig. 11A, E), while Monkey B showed a consistent and significant increase throughout the experiment (day 22: $p = 0.0004$; day 64: $p = 0.0008$). This was expected, as Monkey B's Synergy A relied on FDP and PL to compensate for the loss of FDS function (Fig. 11I, M). Synergy C exhibited a general increase in activity during the post-TT phase in both monkeys (Fig. 11G, O), while Synergy D showed no significant differences in Monkey B and only minor changes in Monkey A (Fig. 11H, P). All statistical comparisons were made against the pre-TT control period using a two-sample t-test with Bonferroni correction ($\alpha = 0.01$).

Taken together, these distinct patterns of aggregated EMG activity, especially the escalating co-activation within the conflicted Synergy B, a known marker of inefficient muscle recruitment (Thoroughman and Shadmehr, 1999; Osu et al., 2002), further illustrate that this early adaptive phase, which coincided with poor behavioral performance (Fig. 5), was characterized by an unstable and inefficient neural control strategy.

Distinct Neural Implementations of a Compensatory Tenodesis Strategy

The final phase of adaptation was characterized by the development of a compensatory tenodesis strategy. This effect describes the passive coupling of finger and wrist movements due to the routing of tendons across multiple joints (Zajac, 1992): because the finger extensor tendons pass over the back of the wrist, actively flexing the wrist passively tightens these tendons, which in turn pulls the fingers into extension (Valero-Cuevas and Hentz, 2002; Cash and Jones, 2011). For Monkey B, we found direct kinematic evidence for the acquisition of this strategy. Post-surgery, the monkey learned to significantly increase finger extension at the metacarpophalangeal (MCP) joint (Fig. 12A) by concurrently flexing the wrist (Fig. 12B; $p < 0.0001$, ANOVA; $\alpha = 0.01$). This coordinated movement pattern is characteristic of an active tenodesis effect. Furthermore, kinematic analysis revealed that this was a gradually learned skill rather than an immediate mechanical consequence. The trial-by-trial coupling between wrist angle and MCP angle (Fig. 13) was initially absent ($R^2 = 0.00$) but strengthened over weeks, peaking in the mid-adaptation phase ($R^2 = 0.58$). This period coincided with the stabilization of grasp aperture (Fig. 5F) and the resolution of the maladaptive neural patterns (Fig. 9). This kinematic strategy was supported by a precise neural implementation. Unlike the scaling strategy observed in Monkey A (see below), Monkey B did not rely on a massive increase in total muscle activity; the aggregated activation of its primary flexor synergy (Synergy A) showed consistent but moderate increases (Fig. 11I, M). Instead, the strategy was one of temporal refinement. The activation profile of Synergy A shifted to increase specifically during the pre-contact phase (Fig. 7G), providing the necessary wrist flexion for the tenodesis grasp. This was achieved by a precise sequential activation of muscles within the synergy, with the wrist flexor component (PL) peaking just before contact and the finger flexor component (FDP) peaking just after (Fig. S2). For Monkey A, which successfully restored its primary extensor synergy, the tenodesis grasp likely served as a similar compensatory driver. While we could not perform a kinematic analysis for this animal due to low-resolution video images, strong evidence for this strategy is provided by the neural data. We observed a clear temporal shift in the activation of its dedicated wrist flexor synergy (Synergy C). The peak of this synergy's activation moved from occurring just after object contact to just before it (Fig. 8C), a re-timing well-suited to enable a tenodesis grasp. This increasing contribution is further supported by cross-correlation analysis, which shows its activation pattern became progressively more similar to that of the pre-TT extensor synergy over time (Fig. 10A; $p < 0.05$, two-sample t-test).

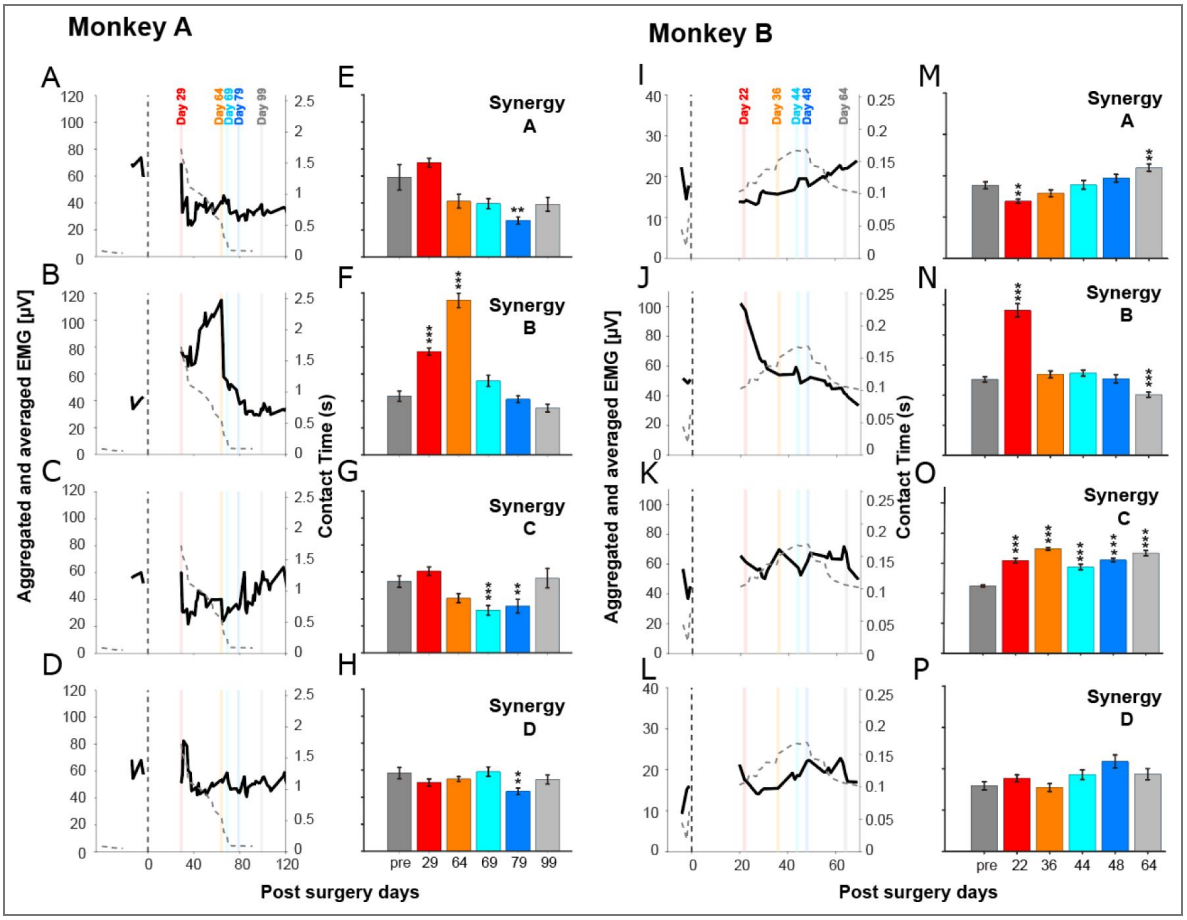

Figure 11. Aggregated and averaged EMG (aaEMG).

Aggregated and averaged electromyography (EMG) activities for the main contributing muscles of each synergy for Monkey A (A-H) and Monkey B (I-P). (A-D, I-L) Time course of aaEMG activity (summed within ±15% task range) plotted over post-surgery days. Black dashed lines on the right y-axis indicate behavioral error metrics. (E-H, M-P) Bar plots showing the mean (± SEM) aaEMG for the pre-TT period ("pre") and the five selected landmark days. Vertical colored bars on the time-series plots indicate the corresponding landmark days. Asterisks indicate significant difference from the pre-TT control period (*p < 0.01, **p < 0.001, ***p < 0.0001; two-sample t-test with Bonferroni correction).

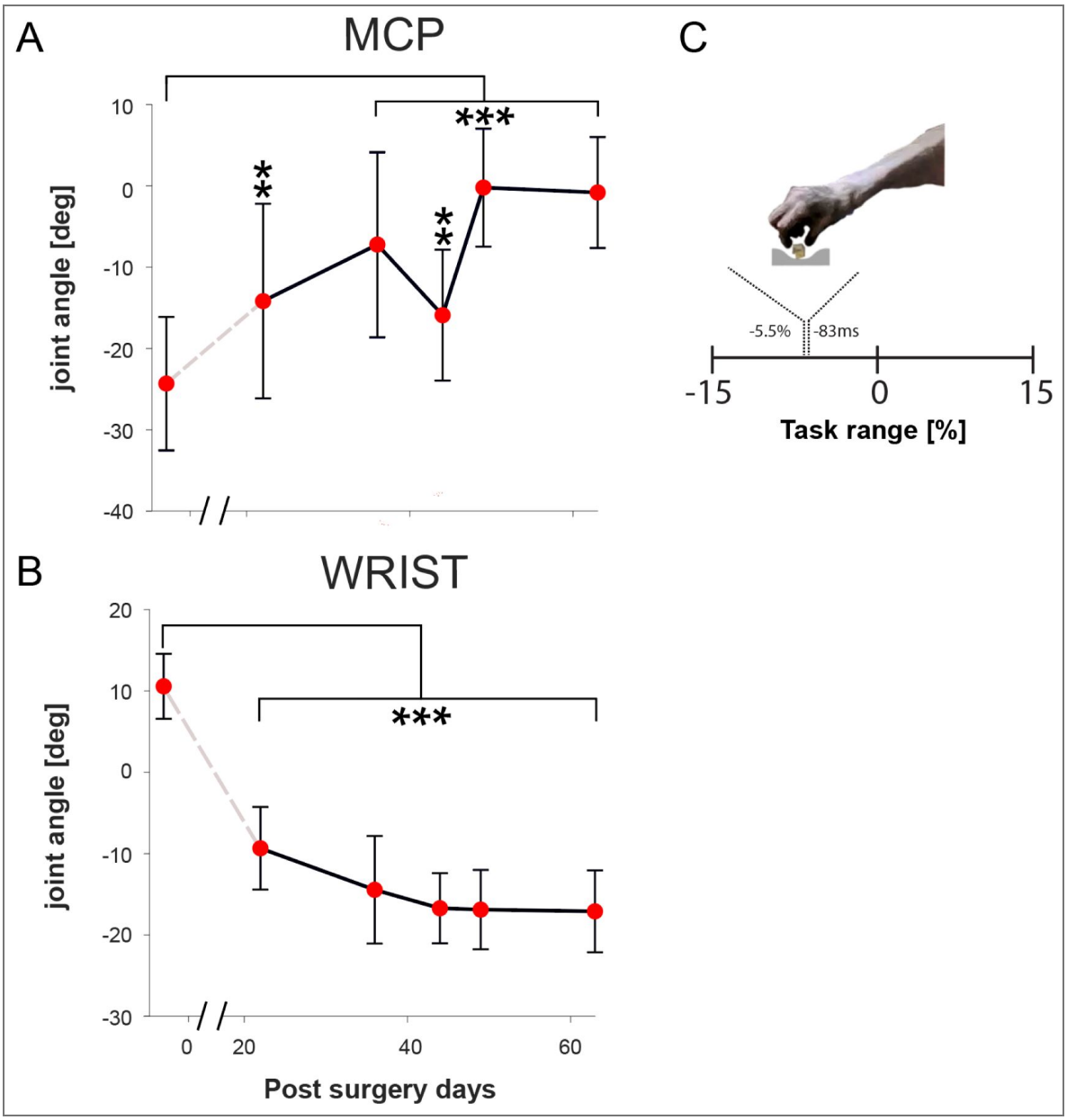

Figure 12. Kinematic analysis of joint angles (Monkey B).

Changes in joint angles (mean of 20 trials ± SD) for each landmark day. (A) Metacarpophalangeal (MCP) joint angle. (B) Wrist joint angle. Asterisks indicate significant difference from pre-TT baseline (**p < 0.001, ***p < 0.0001; ANOVA). (C) Schematic indicating the timing of the kinematic snapshot relative to the task timeline (dotted line; 83 ms before food touch), capturing the hand configuration during the pre-shaping phase.

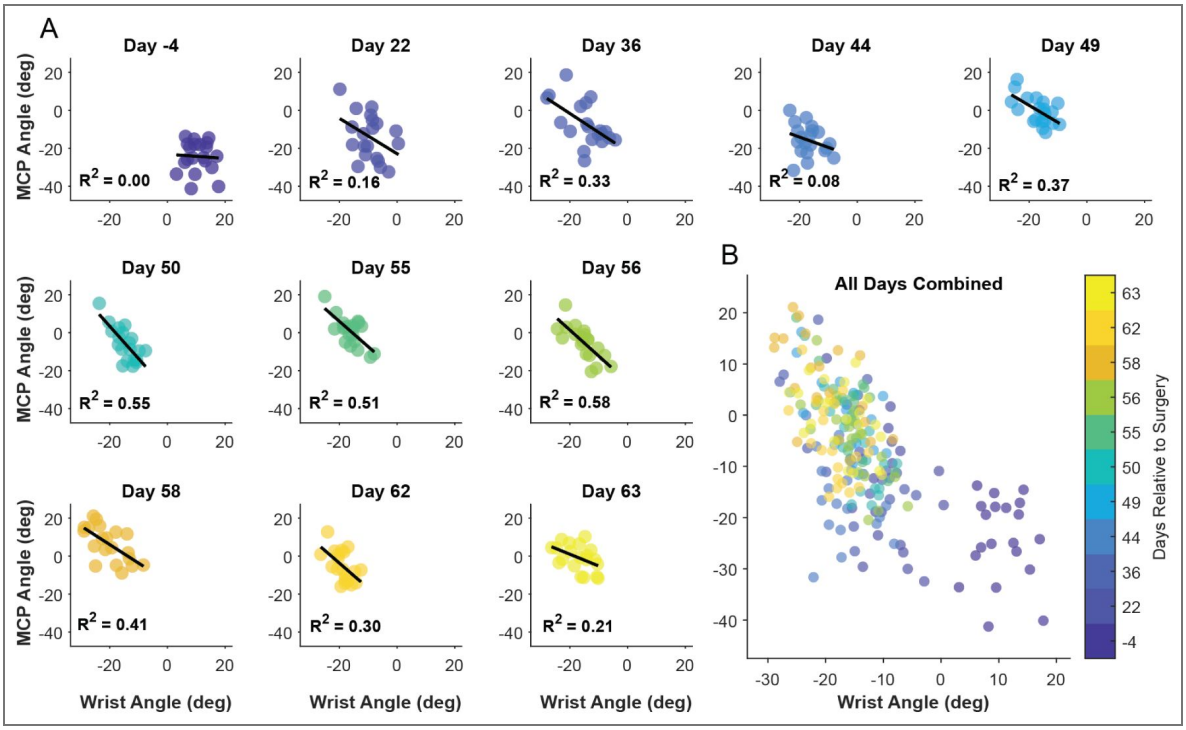

Figure 13. Kinematic analysis reveals gradual refinement of the compensatory tenodesis strategy over time in Monkey

B. (A) Each subplot shows the trial-by-trial relationship between wrist angle (X-axis) and MCP angle (Y-axis) for a single recording day (n=20 trials per day). Points are color-coded based on the day relative to surgery (colorbar). Pre-TT (Day -4), no correlation exists (R^2=0.00). Post-surgery, a negative correlation emerges and strengthens over time, peaking around Day 56 (R^2=0.58), indicating the learned exploitation of the tenodesis effect where wrist flexion predicts finger extension. The tightening of the scatter plots and increase in R^2 over weeks provide direct evidence for a gradual motor skill learning process. (B) All data points combined.

Discussion

The central nervous system's (CNS) response to profound musculoskeletal change is a fundamental problem in motor control. This study sought to determine whether the primate CNS adapts to such change by flexibly modulating stable muscle synergies or by developing more fractionated, independent muscle control. We found that the CNS initially defaulted to a modular strategy, repurposing entire synergies by swapping their activation timings. This simple solution, however, proved to be maladaptive, creating a mechanical conflict that impaired motor function under tendon transfer surgery used in this study. This early maladaptive phase was ultimately resolved through the gradual development of compensatory movements, leading to a "good enough" functional recovery. This multi-stage process, operating on different timescales, highlights the intricate balance between modularity and flexibility in neural adaptation.

Neural Learning, Not Physical Healing, as the Rate-Limiting Factor

A crucial consideration in interpreting our long-term results is the potential confound of the tendon's physical healing process. However, the surgical technique employed, a multi-weave Pulvertaft transfer, is designed to provide immediate mechanical strength comparable to that of a native tendon (Graham et al., 2023). While fibrous integration matures over approximately six weeks, the repair was biomechanically sound from the beginning. This allows us to conclude that the prolonged, multi-month recovery period, characterized by a complex two-phase neural reorganization, was not limited by the tendon's force-bearing capacity but rather reflects the significant challenge of a purely neural learning process.

The CNS Defaults to a Modular Strategy, Leading to a Maladaptive Conflict

Our primary finding provides a direct answer to the question posed in the introduction: the CNS adapted to the tendon transfer not by developing fine-grained, fractionated control, but by implementing a modular strategy by repurposing entire co-activation modules (Overduin et al., 2008; Berger et al., 2013; Bizzi and Cheung, 2013; Takei et al., 2017). The initial and most immediate neural change was a wholesale swap of the temporal activation patterns of the primary flexor and extensor synergies (Synergy A and B). The fact that the spatial structure of all four synergies remained remarkably stable throughout the months-long experiment (Fig. 7I, S6), in the face of drastically altered biomechanics, strongly supports the hypothesis that these synergies represent stable, neurally constrained building blocks (d'Avella et al., 2003; Bizzi and Cheung, 2013; Takei et al., 2017). While our baseline analysis (Fig. 7I) confirmed that natural variability is negligible (>0.99 similarity), the specific, transient structural deviations observed post-surgery (e.g., in the compensatory wrist flexor Synergy C) suggest that the CNS retains a limited capacity to fine-tune the internal structure of these modules when driven by strong functional demands. Consequently, the distinct adaptive patterns observed in individual non-transferred muscles (e.g., FCR, PL in Monkey A) likely reflect this task-specific tuning of secondary synergies, rather than a breakdown of modular control.

Our result indicated that this modular approach is likely the default strategy. One potential reason is that modulating pre-existing modules may be computationally simpler and metabolically less costly than developing entirely new, fractionated control patterns (Flash and Sejnowski, 2001; Bizzi and Cheung, 2013). The latter would require extensive synaptic plasticity, potentially involving cortical remapping to selectively uncouple previously co-activated muscles (Kitago and Krakauer, 2013). Alternatively, or perhaps complementarily, the preservation of synergies may reflect inherent constraints on neural plasticity, suggesting that the underlying neural circuits encoding these modules are relatively immutable, even when faced with significant changes in peripheral mechanics (Makin and Krakauer, 2023). Regardless of the underlying reason, be it computational efficiency, constraints on plasticity, or both, the CNS appears to prioritize modulating the activation of existing modules when dealing with acute alterations to the musculoskeletal system.

However, this adherence to established synergy structures created a fundamental conflict. Activating the original extensor synergy (Synergy B) after the transfer now inevitably co-activated the surgically transferred EDC, which functioned mechanically as a flexor, alongside non-transferred muscles like ED23 and ECU, which remained anatomical extensors. This internal mechanical antagonism appears to be the root cause of the early maladaptive phase. This interpretation is supported by two key lines of evidence from our results. First, the period of severe behavioral impairment, characterized by off-target reaching and inefficient grasping (Fig. 5B, E), occurred precisely when this flawed "swap" strategy was active. Second, the aggregated EMG activity revealed a sustained and significant increase in the total activation of the conflicted Synergy B in Monkey A (Fig. 11B, F), which we interpret as an energetically costly effort to overcome the internal mechanical antagonism. This scenario can be viewed through the lens of optimal control and cost-benefit analysis, where a cost function is minimized (Wolpert, 1997). The initial "swap" strategy, while computationally cheap to select, incurred an unacceptably high operational cost in terms of both poor task performance (high error) and what was likely excessive energy expenditure. We hypothesize that this profoundly unfavorable cost-benefit ratio likely served as the critical error signal that drove the CNS to abandon this initial strategy.

Resolution Through Slower Compensatory Adaptations

The CNS did not persist in the failed swap-based strategy. The high metabolic and computational cost of activating a mechanically conflicted synergy likely triggered the second rapid adaptation: the "switch-back" of synergy activation timings toward their original patterns (Fig. 7, 9). This rapid reversion, occurring over just a few days, is characteristic of an error-based learning mechanism, a form of adaptation that is profoundly impaired by cerebellar damage across a range of tasks, including adaptation to force fields (Smith and Shadmehr, 2005), prismatic shifts (Martin et al., 1996), and split-belt treadmills (Morton and Bastian, 2006). It is plausible that the CNS operates with an implicit threshold for an acceptable cost/performance ratio; once the persistent task failure and high muscular co-contraction of the swap strategy exceeded this threshold, a swift recalibration was initiated. This reversion, despite the remaining mechanical antagonism from the transferred tendons, represents a "good enough" solution where functional success is prioritized over perfect efficiency (Mussa-Ivaldi and Bizzi, 1995; Ranganathan et al., 2013; Gijsberts et al., 2014). Our quantitative analysis supports this interpretation: while the CNS successfully restored the temporal structure of the motor commands (high cosine similarity), it did not perfectly replicate the pre-surgery state. As shown in Figure S8, significant differences in activation amplitude persisted in specific phases of the movement, and permutation tests confirmed the profiles remained statistically distinct. This suggests the system settled into a stable, functional attractor that was sufficiently close to the original manifold to execute the task, without expending the computational or metabolic cost required for a perfect restoration. The rapid timescale of this change is highly consistent with the cerebellum's proposed role as a forward model, predicting the sensory consequences of motor commands and driving rapid learning in response to sensory prediction errors (Popa et al., 2016). Our lag analysis (Fig. S2) confirmed that the timing of motor commands fluctuated significantly before stabilizing.

Crucially, this switch-back to a less conflicted state, presumably representing the involvement of the error-based learning process, was likely enabled only by the concurrent development of slower, compensatory strategies that provided an alternative means to achieve the task goal. The primary compensation was a learned use of the tenodesis effect. Over weeks, the monkeys gradually increased the activation of the wrist flexor synergy (Synergy C) during hand opening. This wrist flexion biomechanically generates passive finger extension (Zajac, 1992; Cash and Jones, 2011), providing a viable new method for hand pre-shaping. This learned, compensatory behavior, confirmed by kinematic analysis (Fig. 12), ultimately allowed the CNS to abandon the maladaptive synergy swap. This gradual, exploratory process is distinct from the following rapid adaptation and represents a form of motor skill acquisition, a process which may be associated with plasticity in cortical structures like the motor cortex and basal ganglia. (Kitago and Krakauer, 2013).

A Multi-Timescale Model Reconciles Smooth Behavioral Recovery and Abrupt Neural Reorganization

The apparent paradox between the smooth, gradual recovery of motor function and the abrupt, switch-like reorganization of the underlying neural control strategy suggests that adaptation is not a single process. Instead, we propose it results from the interaction of at least two distinct adaptive systems operating in parallel on different timescales, a concept aligned with established two-state models of motor learning (Smith et al., 2006a; Trewartha et al., 2014).

We map the gradual acquisition of the compensatory tenodesis strategy to the slow process of this model. This iterative component is responsible for building the robust, stable motor skills necessary for long-term recovery. In contrast, we propose that the fast process drives the initial 'swap' strategy and its subsequent abandonment. This system appears to be sensitive to immediate performance errors and metabolic costs, triggering the rapid 'switch-back' to the original synergy timings (recalibration) once the initial strategy proves inefficient.

The critical insight from our data lies in the interaction between these timescales. We propose that the slow system effectively 'gates' the fast system: the abrupt neural reorganization (the switch-back) is likely not an independent event, but a transition enabled only when the slow learning (tenodesis) reaches a "good enough" threshold to support function. This hierarchical interaction resolves the tension between the smooth behavioral curve and the sharp neural transition, ensuring a stable long-term motor plan (Fig. 14).

Broader Implications and Limitations

Mechanisms of Neural Adaptation

Our findings of a multi-timescale adaptation process involving stable muscle synergies resonate with, yet also extend, previous work on motor learning. Early studies in primates demonstrated a capacity for eventual positive functional readaptation after nerve crossing, moving beyond the initial maladaptive reversals also seen in our monkeys (Sperry, 1947). However, EMG studies in human patients suggest this adaptation may be incomplete, as original 'old' muscle activation patterns often persist alongside newly learned ones (Illert et al., 1986). This aligns with our observation of synergy timing modulation rather than structural reorganization, a finding strongly supported by 'virtual surgery' studies indicating the CNS preferentially adapts by recombining existing motor modules (Berger et al., 2013).

Biomechanical Constraints and Sensory Feedback

The maladaptive conflict ('arms race') observed during the early phase may be exacerbated by peripheral biomechanical factors. Rodent models show that epimuscular myofascial force transmission can cause transferred muscles to generate unexpected antagonistic forces depending on joint angle (Maas and Huijing, 2012). Such biomechanical conflicts likely contributed to the cost and ultimate abandonment of the initial swap strategy. Furthermore, the initial, rapid synergy swap may be linked to a 'sensory surprise' from altered proprioceptive feedback, driving a fast but flawed response (Kitazawa et al., 1995; Martin et al., 1996; Smith et al., 2006b; Edwards et al., 2012; Petitet et al., 2018). This multi-level network reorganization presents a more complex challenge than the gain modulation within single or specific CNS pathways seen in studies of spinal reflex conditioning (Thompson and Wolpaw, 2014). A comprehensive model must ultimately connect the global synergy reorganization with these local, interacting feedback loops, considering factors such as the roles of spinal reflex pathways (Smith et al., 2006c) and fusimotor drive (Vallbo et al., 1979; Hospod et al., 2007).

Task-Dependent Differences. The observation that both monkeys, engaged in both a highly controlled learned task and a more naturalistic grasping task, showed similar adaptive patterns strengthens the generalizability of our findings (Berniker et al., 2013). However, the difference in adaptation rates likely reflects the distinct constraints of these tasks. Monkey A's precision task required exact force vector production, potentially prolonging the neuromuscular conflict. In contrast, Monkey B's naturalistic task allowed for more flexible kinematic solutions, such as the

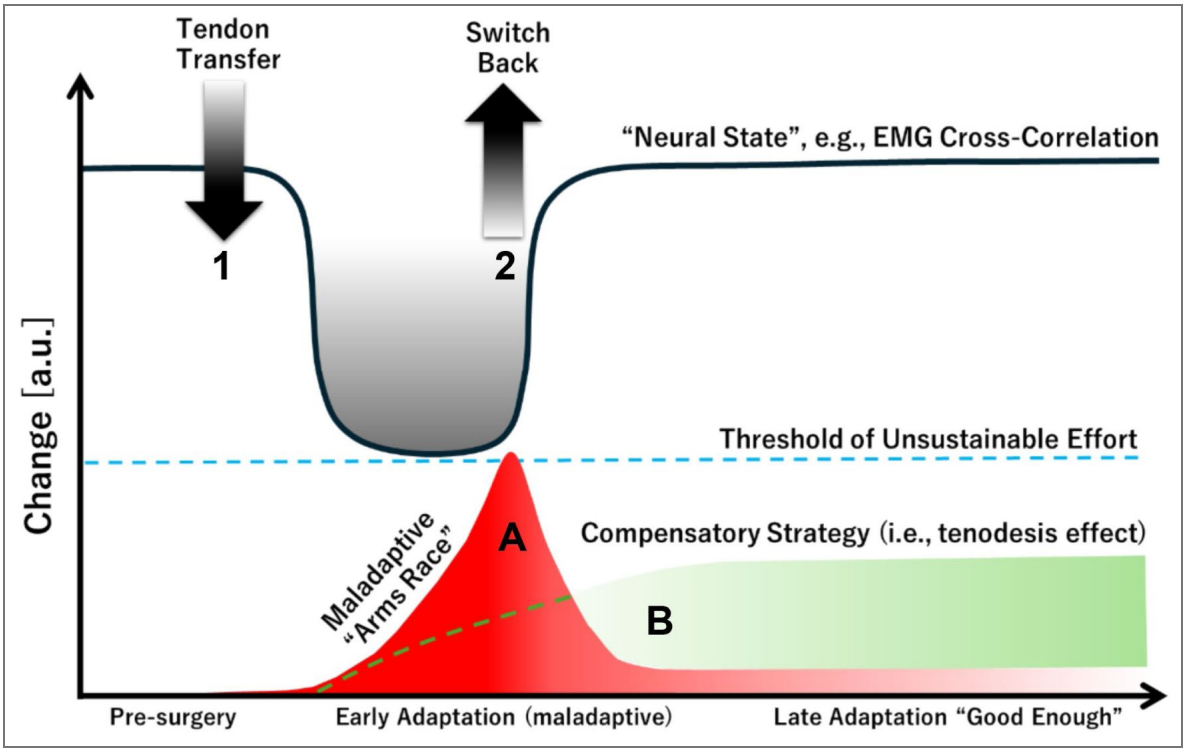

Figure 14. A Proposed Model of Multi-Timescale Adaptation Following Tendon Transfer.

This schematic illustrates the hypothesized interaction between fast and slow adaptive processes driving recovery. The initial Tendon Transfer triggers a rapid but maladaptive 'swap' of motor commands (Fast Adaptation 1), leading to a maladaptive state. During this phase, two slower processes are hypothesized to occur in parallel: a costly 'arms race' within the conflicted synergy (Slow Process A, red curve) and the gradual development of a functional compensatory strategy (Slow Process B, green curve). When the 'arms race' reaches a threshold of unsustainable cost (dashed blue line), a second Fast Adaptation ('Switch-Back', 2) is triggered. This allows for the abandonment of the flawed strategy and the adoption of a stable, 'good enough' solution, which is now supported by the newly learned compensatory strategy. The gray line represents the observed neural data (e.g., cross-correlation coefficients of electromyography and temporal activation profiles of muscle synergies), which reflects this two-phase process.

tenodesis grasp, to be discovered and employed more rapidly. This suggests that while the core neural mechanism (swap-and-revert) is conserved, the timescale of its resolution is sensitive to task constraints.

Motor Memory and Unlearning

Our paradigm raises critical questions about the distinction between unlearning a maladaptive strategy and relearning a functional one (Kitago et al., 2013). The disappearance of the initial "swap" strategy could be due to passive decay, active inhibition (extinction), or interference from a new, stronger memory (Villalta et al., 2013). The literature increasingly suggests that unlearning is an active process, and that the new, successful compensatory strategy likely supplants the maladaptive one through interference. Our results lend weight to this view, suggesting functional recovery is a process of competitive memory formation.

Future Directions

A valuable future direction would be to combine the empirical findings of this study with theoretical biomechanical modeling. A subject-specific musculoskeletal model could provide a more precise mapping of how the tendon transfer altered the biomechanical plant. Integrating these empirical and theoretical approaches represents a critical next step in understanding the complex interplay between biomechanics and neural adaptation (Nakajima et al., 2023).

Implications for Sensorimotor Rehabilitation

These findings may hold implications for sensorimotor rehabilitation. The observation of a distinct maladaptive phase followed by compensation and recovery suggests a staged approach could be beneficial (Hatem et al., 2016; Kakavas et al., 2025). An early phase of therapy might focus on minimizing sensory prediction errors caused by the altered proprioceptive feedback, and reducing maladaptive responses through techniques aimed at integrating the altered body schema (e.g., using visual feedback or task-oriented practice) (Nudo et al., 1996; Takeuchi and Izumi, 2012; Zeiler and Krakauer, 2013; Foell et al., 2014; Levin et al., 2015; De Nunzio et al., 2018; Sattin et al., 2023; van Vliet et al., 2023). This stage would guide the fast, error-driven learning system. A later phase could then employ task-specific training to promote effective compensatory strategies, facilitating the abandonment of maladaptive patterns and the consolidation of a stable motor strategy (Murata et al., 2008; Maier et al., 2019). This second stage engages the slow, skill-acquisition system by creating a rich, problem-solving environment. Finally, a third stage would focus on intensive, high-repetition practice to automate the new functional motor plan, making it robust for real-world use through dosage and generalization (Winterbottom and Nilsen, 2024). This neurobiologically-informed staging, guiding fast adaptation, then facilitating slow skill learning, then driving consolidation, may offer a more logical and effective path to functional recovery.

Methods

Animals

Data were collected using two male macaque monkeys (*Macaca fuscata*; Monkey A: 7.8 kg and Monkey B: 9.9 kg) purpose-bred at the National Bioresource Project (NBRP). They were kept in custom-made primate cages, allowing for potential pair housing. Both monkeys were trained to perform a simple grasping task. During experimental recordings, the monkeys were seated in a primate chair without further restraint. Their head movement remained unrestricted at all times.

Procedures

All procedures were designed to minimize discomfort and pain and approved by the institutional Animal Care and Use Committees at the National Center of Neurology and Psychiatry (NCNP), Tokyo, Japan. Details of the surgical operations, experimental setup, and procedures for electromyography (EMG) recordings have been previously described (Takei and Seki, 2010).

EMG implant surgery

Both animals were familiarized with the experimental setup and trained to perform the behavioral task prior to surgery. After an initial training period, EMG electrodes were chronically implanted subcutaneously into several muscles of the left forearm including the FDS, FDP, and EDC (Figs. 1, 3C, and 4C). Individual muscles were localized and confirmed using electrical microstimulation before implanting EMG electrodes chronically by two methods. For muscles involved in the crossed tendon transfer procedure, muscle fascia was cut and EMG wires with looped ends were placed on top of the muscle belly. These were then secured by reclosing the fascia with absorbable suture threaded through the loop (AS-361, stainless-steel Cooner wire, Conner Wire Co., Chatsworth, CA, USA). All other muscles were directly implanted into the muscle belly using a 22-gauge hypodermic needle. Each wire was threaded into the needle tip, folded back along the shaft, and inserted into the muscle before carefully retracting the needle. Electrode separation for bipolar recordings was approximately 5–10 mm. Note that some EMG recording sites were lost over time. Surgical procedures were carried out under deep general anesthesia (sevoflurane 1.5 to 2.5% in 2:1 O2/N2O) and with full aseptic precautions. Heart rate, blood pressure, body temperature, and blood oxygen saturation were monitored throughout surgery. Analgesics and antibiotics were administered intramuscularly for at least one week postoperatively.

Tendon-Transfer Surgery

After a minimum four-week recovery period from EMG implant surgery, TT surgery was performed. The FDS and EDC tendons were cut as distally as possible (immediately below and above the wrist for FDS and EDC, respectively) to avoid damaging the Golgi tendon organ located near the junction between the muscle fibers and tendon (Schoultz and Swett, 1972; Jami, 1992). Tendons were then guided either through the gap between the radius and ulnar bone (Monkey A), or around the wrist and then re-attached to the tendon of the antagonist muscle using a tendon graft harvested from the plantaris tendon of the lower limb (Monkey B; EDC → FDS: direct connection; and FDS → EDC: tendon grafting). The tendon coaptation was performed using a Pulvertaft weave technique (weaves > 2) with high-strength non-absorbable suture material to ensure immediate and robust mechanical stability post-surgery (Graham et al., 2023). This was only necessary in Monkey B since the tendons used for the cross-transfer were too short. This surgical procedure aimed to reverse the primary mechanical actions of the manipulated muscles, making the FDS tendon an effective finger extensor and the EDC tendon an effective finger flexor. The success and nature of this mechanical rearrangement were verified post-operatively via direct muscle stimulation (see Methods subsection 'Tendon transfer confirmation' and Fig. 2). The general organization and function of the major forearm muscles involved in finger flexion and extension in *Macaca fuscata* are broadly comparable to those in humans (Vanhoof et al., 2021; Yan et al., 2022).

Surgical procedures were carried out under deep general anesthesia (sevoflurane 1.5 to 2.5% in 2:1 O_2/N_2O) and with full aseptic precautions. Heart rate, blood pressure, body temperature, and blood oxygen saturation were monitored throughout surgery. Analgesics and antibiotics were administered intramuscularly for at least one week postoperatively. Both monkeys wore a plaster cast post-surgery, but its effectiveness was limited (lasting approximately one week).

Tendon transfer confirmation

To verify the success and long-term stability of TT surgery, two procedures (Fig. 2) were implemented. During the first procedure, the monkey was sedated and its arm was secured to a metal frame (Fig.2A). Electrical stimulation was then applied to either the FDS or EDC muscle (50 mA, DS8R, Digitimer, Welwyn Garden City, UK), while ultrasound scans of tendon movements were concurrently captured (SONIMAGE MX1, Konica Minolta, Inc., Tokyo, Japan (Nordez et al., 2009; Dieterich et al., 2017).

Figure 2B shows a sonogram of the FDS muscle and its intramuscular tendons. The left side displays a static image of the FDS muscle at a specific moment, with white arrows indicating the FDS tendon used for measurement. The right side shows staggered images (top white box) of the FDS tendon displacement triggered by muscle stimulation. The lower right inset illustrates the measurement area. The displacement wave area represents the intensity of muscle contraction, and was calculated by measuring the average duration (a, in seconds) and amplitude (b, in cm) of three successive waves. The area (a*b/2) and regression line for FDS (red) and EDC (blue) ($R^2 > 0.5$ for FDS) for days 0, 7, and 105 post-TT are shown (Fig. 2C). The results suggest that the muscle contractions induced by direct electrical stimulation remained nearly constant.

For the second procedure, high-speed videos (37U Series Color Industrial Camera, The Imaging Source, Charlotte, NC, USA) of the monkey's finger movements were recorded while electrically stimulating the FDS or EDC. Markers were placed on the nails of the index, middle, and ring fingers (Fig. 2A) to measure finger displacement in xyz-dimensions using DeepLabCut software (Mathis et al., 2018; Nath et al., 2019). The sum of Euclidean distances of each marker from the origin of the three-dimensional (3D) coordinate system was computed as a scalar quantity. Post-surgery, movement along the z-axis reversed, indicating a shift from finger flexion to extension due to TT (Fig. 2D; blue: pre-TT on surgery day, dark brown: post-TT on surgery day, light brown: 1 wk post-TT, and red: 3 wk post-TT). The scalar quantities of each finger did not significantly change during muscle stimulation on days 0-, 7-, and 105-days post-TT (Fig. 2E), suggesting there was no postoperative tendon rupture or slackening.

Data recordings

EMG signals were recorded using the AlphaLab SnR system (Alpha Omega Engineering, Hamerkava St. 6, Ziporit Industrial Zone, P.O. Box 810, Nof HaGalil (Nazareth Illit) 1789062, Israel), displayed online and then stored on a hard drive for later off-line analysis using MATLAB (MathWorks, Natick, MA, USA). Data were recorded at 11 kHz and processed for analysis as follows. 1. Down-sampled to 5 kHz; 2. 50 Hz high-pass filtered (6th order Butterworth filter); 3. rectified; 4. 20 Hz low-pass filtered (6th order Butterworth filter); and 5. down-sampled to 100 Hz. Behavioral task events were recorded as transistor–transistor logic (TTL) signals using the AlphaLab SnR system. Monkey behavior was further recorded by two cameras (Sanyo VPC-WH1, 60 fps [Sanyo, Osaka, Japan]; and Casio EX-100F, 240 fps [Casio, Tokyo, Japan] for monkeys A and B, respectively) from two different angles (top and side view). The images were later used to detect additional behavioral events (contact time with the object and pull onset for Monkey A; and food touch and food lift onset for Monkey B), and detection of possible changes in the animal's general movement pattern. Kinovea software was used for this video analysis (free and open-source software; *https://www.kinovea.org/*).

Behavioral task

Before and after EMG surgery, the monkeys were trained on a simple grasping task that involved a small object attached to a rod (Fig. 3A for Monkey A; and Fig. 4A for Monkey B). For Monkey A, object 1 was a small rod placed between two side walls encouraging the monkey to grasp the rod with a precision grip using the tips of the index finger and thumb (controlled grasp). The force used to compress the spring while pulling was low and the distance moved short. Object 2 had to be grasped in the same way. However, the force to compress the spring was higher and the distance moved longer (object 1: 300 cN, 4 mm; and object 2: 800 cN, 30 mm). The monkey was asked to grasp and hold the objects for approximately 300–500 ms (Fig. 3A–D). After completing the trial, the monkey was rewarded with a piece of fruit that had to be taken from the experimenter's palm. The task sequence for Monkey A ranged from object 1 hold onset to object 2 hold offset (Fig. 3C, D; and 'Data Analysis' below). For Monkey B, object 1 was a small rod that was grasped and pulled (300 cN, 4 mm) using a lateral prehension grip (like using a door key), and resembling a power grip rather than a natural grasp. However, instead of grasping object 2, Monkey B picked up a piece of fruit from an allocated location. In doing so, the monkey had to

cross the path of a photo cell which was detected by the recording system (Fig. 4A–D). The task sequence to be analyzed for Monkey B ranged from object 1 hold onset to food touch, which was indicated by a LED (Fig. 4C, D; and 'Data Analysis' below).

For Monkey A, the task sequence was as follows (Fig. 3B; and Supplementary Video S1). From a starting position in front of the monkey, it had to lift its arm and move towards object 1, grasp, pull, and then hold the object for 500 ms. Immediately after releasing object 1, Monkey A proceeded to move its hand towards object 2, which was located to the right of object 1. Again, the monkey had to grasp, pull, and then hold the object for another 500 ms. Each hold period was accompanied by an audio signal which stopped once the hold duration was sufficient. After completing the task, which was signaled by another acoustic signal, the monkey was rewarded with a piece of fruit presented by the experimenter and taken by the monkey.

For Monkey B, the first part of the sequence was identical. However, after releasing object 1, Monkey B was required to pick up a piece of fruit from an allocated location (Fig. 4A, B; and Supplementary Video S5). In doing so, the monkey passed a photocell in front of the food well. This event was detected by the recording system and a video camera (a red LED triggered by activation of the photocell). For the analysis, only object 1 and the food grasp were considered in monkeys A and B, respectively.

Data analysis

EMG analysis

EMG data were normalized to the average time for each monkey to complete a trial (object 1 hold onset ➔ object 2 hold offset/LED offset = 100%). Data were cropped and aligned according to the time stamps (Obj1 hold offset ± 15%; and LED onset [food touch] ± 15% for monkeys A and B, respectively). Recorded EMGs from the pre- and post-tendon surgery period were averaged for each recording and compared over experimental sessions. For Monkey A, FDS and EDC were analyzed both pre- and post-TT. For Monkey B, FDS and EDC were analyzed pre-TT, but only EDC was analyzed post-TT due to signal deterioration.

Both monkeys required time to recover from surgery. Post-TT recordings were resumed once the monkeys were able to perform the task independently (i.e., without assistance from the experimenter) and met specific trial count criteria (starting 29 and 20 days post-surgery for monkeys A and B, respectively). Post-operative recording sessions were conducted frequently throughout the recovery period, though not at fixed daily intervals, reflecting the practical constraints of long-term behavioral experiments (e.g., animal cooperation, experimental scheduling) and the aim to capture data during key phases of adaptation. Within any given session included in the analysis, behavioral (video) and EMG data were collected concurrently. To be included in the behavioral analyses (e.g., grip formation times, off-target reaching, kinematics), a session required a minimum of 20 successful trials. For the more demanding muscle synergy analyses, a higher threshold of at least 100 successful trials was required to ensure robust factorization. This difference in criteria may have resulted in slightly different sets of recording days being represented across behavioral versus synergy-related figures. After tendon surgery, EMG signals for FDS, FCU, and FCR deteriorated in Monkey B. Therefore, there is no experimental data for these muscles in this monkey and they were excluded from the muscle synergy analysis.

Synergy analysis

The EMG envelopes obtained from pre-processing raw EMG data were divided by the mean value to normalize activity. Muscle synergies were then extracted for each session using NMF (d'Avella et al., 2003). NMF decomposes the EMG data matrix M, as a product of two matrices C and W:

$$M = CW^T + re = \Sigma c_i w_i^T + re$$

where the vector wi and column of matrix W are muscle synergies; the vector ci, and column of matrix C are their temporal coefficients; and re represents the residuals. Multiplicative update rules were used for decomposition (Lee and Seung, 1999). Updating matrices for

decomposition from 20 different random initial matrices was started, and factorization results with least residuals among the 20 results were used. To improve robustness of the muscle synergies, one set of muscle synergies was extracted from EMG data of multiple trials of each day. A k-fold cross validation was used, with k = 4 i.e., EMG data set of multiple trials during the day was split into four data sets, in which three data sets were for training and one data set was for testing. Synergy matrix W was calculated from three training data sets using NMF, and then a coefficient matrix C was calculated by decomposing the EMG matrix M of the test data set with a fixed W matrix of the training data set. This operation was repeated by changing the test data set for each four data sets. Finally, the extracted four C matrices and four W matrices were averaged to obtain daily synergies.

The number of synergies was determined as the number where VAF exceeded a threshold. This threshold was set as 0.8. To clarify the effect of TT, the number of synergies for each monkey was determined, assuming that trial-by-trial variation in synergies within the same monkey was small. MATLAB 'nnmf' function was used for NMF.

To determine whether the weights of muscle synergies changed after TT, the following procedure was used. First, the average of each pre-TT spatial synergy was calculated and used as control data to calculate the cosine distance for all post-TT spatial synergies. This generated four distance relationships for each pre-TT synergy. If the change in spatial synergy before and after TT was small, then only one of the four cosine distances (e.g., synergy A before TT and synergy A after TT) should be significantly smaller. Two-way ANOVA was conducted using the type of synergy and session as factors for the cosine distance. The significance of synergy pairs was identified using the Bonferroni post-hoc test.

Quantitative Comparison of Synergy Profiles

To quantify the degree of 'reversion' in the late adaptation phase, we compared the synergy activation profiles from the pre-surgery period with those from the final recording day using three distinct metrics. First, Cosine Similarity was calculated to assess the similarity in the shape of the temporal profiles independent of amplitude. Second, a Permutation Test (n=10,000 iterations) was performed to test whether the specific trajectory of the post-surgery profile was statistically distinguishable from the pre-surgery distribution. Third, to identify specific phases of the task where activation differences persisted, we conducted a point-by-point Wilcoxon rank-sum test at each time point of the normalized task cycle, applying a Bonferroni correction for multiple comparisons.

Cross-correlation analysis

Cross-correlation analysis was performed to examine the similarity between pre-and post-surgery EMG signals as well as temporal activation profiles of extracted muscle synergies. For the EMG signal analysis presented in Figure 6, the cross-correlation coefficient at zero-time lag was calculated. For the synergy analysis presented in the main figures (Figs. 9, 10), the cross-correlation coefficient at zero-time lag was calculated using MATLAB (MathWorks, corrcoef function) to quantify similarity without temporal shifts. These zero-lag coefficients were plotted over experimental sessions. In a supplementary analysis, we also computed the cross-correlation allowing for variable time lags using MATLAB's xcorr function (normalized using the 'coeff' option). From this, we extracted the specific time lag that yielded the maximum cross-correlation coefficient (optimal lag) for each session for both the muscle synergies (Supplementary Figure S9) and the individual EMG signals (Supplementary Figure S1). In this analysis, a positive lag indicates that the post-surgery activation profile is delayed (occurs later) relative to the pre-surgery baseline, while a negative lag indicates it is advanced (occurs earlier).

Based on cross-correlation analysis, five 'landmark days' were identified for further analysis (Fig. 6P). These days represent distinct stages in the recovery process and excluded pre-TT control data. The first landmark day was chosen from one of the initial recording sessions after TT surgery (days 29 and 22 in monkeys A and B, respectively) when the cross-correlation coefficients had changed significantly compared with control data. The second day was then chosen from a time period just before the switch-back, when the cross-correlation coefficients had started to return to

their original values (days 64 and 36). Another day was then picked from the period when the coefficients were still changing significantly (days 69 and 44) and before starting to saturate. At this point the next day was defined (days 79 and 48). Finally, the final landmark day was chosen from one of the last recording sessions when the behavior had fully recovered (days 99 and day 64 for monkeys A and B, respectively).

Behavioral analysis

To examine behavioral recovery, the duration, onset, and offset of object and food grasps were analyzed. Event times extracted from the video analysis were used for alignment of EMG data and subsequent cross-correlation and synergy analyses, along with recorded event TTL signals. For each experimental session, the first 20 trials of each video recording were analyzed. In Monkey A, the following events were detected and in-between times stored in ms: touch onset, pull onset, and hold onset (resulting in grasp duration and pull time) for object 1 and object 2. In Monkey B, the following events were detected and in-between times stored: touch onset, pull onset, and hold onset (resulting in grasp duration and pull time) for object 1; and for the food grasp component of the task, LED onset, food-touch onset, food-lift onset, LED offset, and movement end (contact of food with mouth).

Contact times (touch onset ➔ pull onset) for Monkey A were plotted in ms (mean ± SD) over number of days from tendon surgery for object 1. For Monkey B, contact times with food (food-touch ➔ food-lift onset) were plotted in ms (mean ± SD).

ANOVA was performed to compare control data recorded before and after tendon surgery. In total, 5 and 3 control sessions vs. 35 and 22 experimental sessions were used for analyses in monkeys A and B, respectively.

To quantify and compare the baseline behavioral variability of these metrics, we analyzed all pre-TT trials for each animal's respective tasks. We calculated the Coefficient of Variation (CV), defined as the standard deviation divided by the mean, for each metric (grip formation time, pull time, and grasp aperture). To formally test the difference in variance for the grip formation task (Fig. 5A, D), we used the non-parametric Ansari-Bradley test. To quantify the observed off-target reaching behavior, video footage was analyzed and the means of 10 consecutive trials calculated for each session as follows. For Monkey A, time spent within a specific spatial window covering the area behind and between the two objects was measured; the monkey passed through this space almost exclusively while exhibiting the impairment (see Fig. 3E, crossing of the yellow dotted line). In Monkey B, the time spent in contact with the rear plate of the object was measured (see Fig. 4E).

In addition to the primary behavioral metrics, we performed a more detailed video analysis of movement kinematics and performance. For Monkey A, we quantified the 'pull time' for each trial, defined as the duration from the moment the monkey started pulling the object to the moment hold onset. For Monkey B, we quantified the 'grasp aperture'. This was defined as the distance between the tips of the index finger and thumb, measured just before the monkey made contact with the food pellet.

Joint kinematics analysis

To determine whether compensatory movements occurred, steady state changes in joint angles were examined before and after recovery. Using DeepLabCut (Mathis et al., 2018; Nath et al., 2019), key points on the fingers and wrists were tracked from experimental videos. From the obtained key points, the vector v_2 connecting the wrist and fingers and vector v_2 connecting the arm and wrist were estimated (Fig. S10). The joint angle θ was calculated as follows:

$$\cos(\Theta) = \frac{v_2 \cdot v_3}{|v_2||v_3|} \rightarrow \Theta = \cos^{-1}\left(\frac{v_2 \cdot v_3}{|v_2||v_3|}\right)$$

To quantify the learning and refinement of the compensatory tenodesis strategy over time, we analyzed the trial-by-trial relationship between wrist and MCP joint angles for Monkey B. For each recorded day, we performed a linear regression between the wrist angle (predictor) and the MCP angle (outcome) across all successful trials (mean of 20 trials ±SD for each

landmark day, taken 83ms before food touch). The strength of the coupling was quantified using the coefficient of determination (R^2). These daily scatter plots and their corresponding R^2 values were visualized to track the evolution of the kinematic coupling from the pre-TT baseline through the post-surgery adaptation period.

Data availability

All data and custom MATLAB code used to generate the figures in this study are available at the GitHub repository: *https://github.com/animalmodel/Philipp_eLife_2025*. For long-term preservation, the code and dataset (including large EMG and Synergy matrices) have been archived at Zenodo (DOI: *https://doi.org/10.5281/zenodo.18030926*).

Acknowledgements

We would like to express our sincere gratitude to Drs. Francisco Valero-Cuevas and Andrea d'Avella for their invaluable comments and constructive suggestions on the earlier version of the manuscript, and Drs Nicholas Schweighofer and Gerald E. Loeb for stimulating discussion. We would also like to thank Dr. Naomichi Ogihara and Prof. Toshiyasu Nakamura for their valuable insights and technical advice on tendon surgery in the hand and forearm of primates. We are grateful to Drs. Kumiko Oida and Chika Sasaki for their medical care of the experimental animals, vital help during surgery, and training of the animals. Lastly, we would like to thank Masahi Koizumi for designing parts of the experimental setup and Drs. Joachim Confais, Shinji Kubota, Saeka Tomatsu, Tatsuya Umeda, and Natsumi Uchida for their support and assistance during the proceeding pilot study. We thank Rachel James, PhD, from Edanz (*https://jp.edanz.com/ac*) for editing a draft of this manuscript. This work was supported by Grants-in-Aid for Scientific Research from the Ministry of Education, Culture, Sports, Science, and Technology of Japan (26120003, 26250013, 15K21754, 19H05724, 19H01092, 23H05488, and 24K21313), the Japan Agency for Medical Research and Development (JP24gm0010009), the Japan Science Technology Agency Precursory Research for Embryonic Science and Technology program, commissioned research (no. 22102) from the National Institute of Information and Communications Technology, and commissioned research by National Institute of Information and Communications Technology (NICT), Japan (all to K.S.). This work is also supported in part by the NSF CRCNS Japan-US 2113096 to K.S. (Subaward PI) and Francisco Valero-Cuevas (PI). The content is solely the responsibility of the authors and does not necessarily represent the official views of the NSF.

Additional information

Author Contributions

R.P. and K.S. designed all experiments and wrote the paper. R.P., Y.H., N.U., and N.O. performed the experiments and analyzed the data. R.P., Y.H., T.O., and K.S. performed the surgeries. T.F. provided conceptual advice and wrote the paper. All authors reviewed the results and approved the final version of the manuscript.

Funding

Funder	Grant reference number	Author
MEXT | Japan Society for the Promotion of Science (JSPS)	26120003	Kazuhiko Seki
MEXT | Japan Society for the Promotion of Science (JSPS)	26250013	Kazuhiko Seki
MEXT | Japan Society for the Promotion of Science (JSPS)	15K21754	Kazuhiko Seki
MEXT | Japan Society for the Promotion of Science (JSPS)	19H05724	Kazuhiko Seki

MEXT | Japan Society for the Promotion of Science (JSPS)	19H01092	Kazuhiko Seki
MEXT | Japan Society for the Promotion of Science (JSPS)	23H05488	Kazuhiko Seki
MEXT | Japan Society for the Promotion of Science (JSPS)	24K21313	Kazuhiko Seki
Japan Agency for Medical Research and Development (AMED)	JP24gm0010009	Kazuhiko Seki
MEXT | Japan Science and Technology Agency (JST)		Kazuhiko Seki
National Science Foundation (NSF)	2113096	Kazuhiko Seki

Author ORCID iDs

Roland Philipp: https://orcid.org/0000-0002-5850-7539
Tetsuro Funato: https://orcid.org/0000-0003-2964-5227
Kazuhiko Seki: https://orcid.org/0000-0002-4262-9590

Additional files

Supplementary information

Supplementary video 1.

Supplementary video 2.

Supplementary video 3.

Supplementary video 4.

Supplementary video 5.

Supplementary video 6.

Supplementary video 7.

References

Berger DJ, Gentner R, Edmunds T, Pai DK, d'Avella A (2013) Differences in Adaptation Rates after Virtual Surgeries Provide Direct Evidence for Modularity. *The Journal of Neuroscience* **33**:12384-12394 https://doi.org/10.1523/jneurosci.0122-13.2013 | PubMed

Berniker M, O'Brien MK, Kording KP, Ahmed AA (2013) An Examination of the Generalizability of Motor Costs. *PLOS One* **8**:e53759 https://doi.org/10.1371/journal.pone.0053759 | PubMed

Bizzi E, Cheung VC (2013) The neural origin of muscle synergies. *Frontiers in Computational Neuroscience Volume* 7-2013 https://doi.org/10.3389/fncom.2013.00051 | PubMed

Bowlus TH, Lane RD, Stojic AS, Johnston M, Pluto CP, Chan M, Chiaia NL, Rhoades RW (2003) Comparison of reorganization of the somatosensory system in rats that sustained forelimb removal as neonates and as adults. *J Comp Neurol* **465**:335-348 https://doi.org/10.1002/cne.10849 | PubMed

Cash DJW, Jones JWM (2011) The role of tenodesis in surgery of the upper limb. *The Journal of Bone & Joint Surgery British Volume* **93-B**:285-292 https://doi.org/10.1302/0301-620x.93b3.25797 | PubMed

Cheung VC, Turolla A, Agostini M, Silvoni S, Bennis C, Kasi P, Paganoni S, Bonato P, Bizzi E (2012) Muscle synergy patterns as physiological markers of motor cortical damage. *Proc Natl Acad Sci U S A* **109**:14652-14656 https://doi.org/10.1073/pnas.1212056109 | PubMed

d'Avella A, Saltiel P, Bizzi E (2003) Combinations of muscle synergies in the construction of a natural motor behavior. *Nature Neuroscience* **6**:300-308 https://doi.org/10.1038/nn1010 | PubMed

Davidson PR, Wolpert DM (2003) Motor learning and prediction in a variable environment. *Curr Opin Neurobiol* **13**:232-237 https://doi.org/10.1016/s0959-4388(03)00038-2 | PubMed

De Nunzio AM, Schweisfurth MA, Ge N, Falla D, Hahne J, Gödecke K, Petzke F, Siebertz M, Dechent P, Weiss T, *et al.* (2018) Relieving phantom limb pain with multimodal sensory-motor training. *J Neural Eng* **15**:066022 https://doi.org/10.1088/1741-2552/aae271 | PubMed

Dieterich AV, Botter A, Vieira TM, Peolsson A, Petzke F, Davey P, Falla D (2017) Spatial variation and inconsistency between estimates of onset of muscle activation from EMG and ultrasound. *Sci Rep* **7**:42011 https://doi.org/10.1038/srep42011 | PubMed

Edwards MJ, Adams RA, Brown H, Pareés I, Friston KJ (2012) A Bayesian account of 'hysteria'. *Brain* **135**:3495-3512 https://doi.org/10.1093/brain/aws129 | PubMed

Flash T, Sejnowski TJ (2001) Computational approaches to motor control. *Curr Opin Neurobiol* **11**:655-662 https://doi.org/10.1016/s0959-4388(01)00265-3 | PubMed

Fleury L, Prablanc C, Priot AE (2019) Do prism and other adaptation paradigms really measure the same processes?. *Cortex* **119**:480-496 https://doi.org/10.1016/j.cortex.2019.07.012 | PubMed

Foell J, Bekrater-Bodmann R, Diers M, Flor H (2014) Mirror therapy for phantom limb pain: brain changes and the role of body representation. *Eur J Pain* **18**:729-739 https://doi.org/10.1002/j.1532-2149.2013.00433.x | PubMed

Gaetz W, Dockstader C, Furlong PL, Amaral S, Vossough A, Schwartz ES, Roberts TPL, Scott Levin L (2023) Somatosensory and motor representations following bilateral transplants of the hands: A 6-year longitudinal case report on the first pediatric bilateral hand transplant patient. *Brain Res* **1804**:148262 https://doi.org/10.1016/j.brainres.2023.148262 | PubMed

Gardenier J, Garg R, Mudgal C (2020) Upper Extremity Tendon Transfers: A Brief Review of History, Common Applications, and Technical Tips. *Indian J Plast Surg* **53**:177-190 https://doi.org/10.1055/s-0040-1716456 | PubMed

Gijsberts A, Bohra R, Sierra González D, Werner A, Nowak M, Caputo B, Roa MA, Castellini C (2014) Stable myoelectric control of a hand prosthesis using non-linear incremental learning. *Front Neurorobot* **8**:8 https://doi.org/10.3389/fnbot.2014.00008 | PubMed

Graham EM, Oliver JD, Hendrycks R, Maglic D, Mendenhall SD (2023) Alternative Tendon Coaptations to the Pulvertaft Weave Technique: A Systematic Review and Meta-Analysis of Biomechanical Studies. *Hand* **18**:446-455 https://doi.org/10.1177/15589447211043213 | PubMed

Green HJ (1997) Mechanisms of muscle fatigue in intense exercise. *J Sports Sci* **15**:247-256 https://doi.org/10.1080/026404197367254 | PubMed

Hatem SM, Saussez G, Della Faille M, Prist V, Zhang X, Dispa D, Bleyenheuft Y (2016) Rehabilitation of Motor Function after Stroke: A Multiple Systematic Review Focused on Techniques to Stimulate Upper Extremity Recovery. *Front Hum Neurosci* **10**:442 https://doi.org/10.3389/fnhum.2016.00442 | PubMed

Hoffmann G, Kamper DG, Kahn JH, Rymer WZ, Schmit BD (2009) Modulation of stretch reflexes of the finger flexors by sensory feedback from the proximal upper limb poststroke. *J Neurophysiol* **102**:1420-1429 https://doi.org/10.1152/jn.90950.2008 | PubMed

Hospod V, Aimonetti J-M, Roll J-P, Ribot-Ciscar E (2007) Changes in Human Muscle Spindle Sensitivity during a Proprioceptive Attention Task. *The Journal of Neuroscience* **27**:5172-5178 https://doi.org/10.1523/jneurosci.0572-07.2007 | PubMed

Hunter DJ, Eckstein F (2009) Exercise and osteoarthritis. *J Anat* **214**:197-207 https://doi.org/10.1111/j.1469-7580.2008.01013.x | PubMed

Illert M, Trauner M, Weller E, Wiedemann E (1986) Forearm muscles of man can reverse their function after tendon transfers: An electromyographic study. *Neuroscience Letters* **67**:129-134 https://doi.org/10.1016/0304-3940(86)90385-x | PubMed

Jami L (1992) Golgi tendon organs in mammalian skeletal muscle: functional properties and central actions. *Physiol Rev* **72**:623-666 https://doi.org/10.1152/physrev.1992.72.3.623 | PubMed

Kakavas G, Brilakis E, Papatzikou M, Malliaropoulos N, Mazeas J, Forelli F (2025) Reverse Linear Neuro Periodization Model for Rehabilitation After Arthroscopic Rotator Cuff Repair: A Narrative Review. *Clinics and Practice* **15**:105 https://doi.org/10.3390/clinpract15060105 | PubMed

Kitago T, Krakauer JW (2013) Motor learning principles for neurorehabilitation. *Handb Clin Neurol* **110**:93-103 https://doi.org/10.1016/b978-0-444-52901-5.00008-3 | PubMed

Kitago T, Ryan SL, Mazzoni P, Krakauer JW, Haith AM (2013) Unlearning versus savings in visuomotor adaptation: comparing effects of washout, passage of time, and removal of errors on motor memory. *Front Hum Neurosci* **7**:307 https://doi.org/10.3389/fnhum.2013.00307 | PubMed

Kitazawa S, Kohno T, Uka T (1995) Effects of delayed visual information on the rate and amount of prism adaptation in the human. *J Neurosci* **15**:7644-7652 https://doi.org/10.1523/jneurosci.15-11-07644.1995 | PubMed

Lee DD, Seung HS (1999) Learning the parts of objects by non-negative matrix factorization. *Nature* **401**:788-791 https://doi.org/10.1038/44565 | PubMed

Levin MF, Weiss PL, Keshner EA (2015) Emergence of virtual reality as a tool for upper limb rehabilitation: incorporation of motor control and motor learning principles. *Phys Ther* **95**:415-425 https://doi.org/10.2522/ptj.20130579 | PubMed

Loeb GE (1999) Asymmetry of hindlimb muscle activity and cutaneous reflexes after tendon transfers in kittens. *J Neurophysiol* **82**:3392-3405 https://doi.org/10.1152/jn.1999.82.6.3392 | PubMed

Luauté J, Schwartz S, Rossetti Y, Spiridon M, Rode G, Boisson D, Vuilleumier P (2009) Dynamic changes in brain activity during prism adaptation. *J Neurosci* **29**:169-178 https://doi.org/10.1523/jneurosci.3054-08.2009 | PubMed

Maas H, Huijing PA (2012) Mechanical effect of rat flexor carpi ulnaris muscle after tendon transfer: does it generate a wrist extension moment?. *Journal of Applied Physiology* **112**:607-614 https://doi.org/10.1152/japplphysiol.01275.2011 | PubMed

Maier M, Ballester BR, Verschure PFMJ (2019) Principles of Neurorehabilitation After Stroke Based on Motor Learning and Brain Plasticity Mechanisms. *Frontiers in Systems Neuroscience Volume* 13-2019 https://doi.org/10.3389/fnsys.2019.00074 | PubMed

Makin TR, Krakauer JW (2023) Against cortical reorganisation. *eLife* **12**:e84716 https://doi.org/10.7554/eLife.84716 | PubMed

Martin TA, Keating JG, Goodkin HP, Bastian AJ, Thach WT (1996) Throwing while looking through prisms. II. Specificity and storage of multiple gaze-throw calibrations. *Brain* **119**:1199-1211 https://doi.org/10.1093/brain/119.4.1199 | PubMed

Mathis A, Mamidanna P, Cury KM, Abe T, Murthy VN, Mathis MW, Bethge M (2018) DeepLabCut: markerless pose estimation of user-defined body parts with deep learning. *Nature Neuroscience* **21**:1281-1289 https://doi.org/10.1038/s41593-018-0209-y | PubMed

Mercuri E, Muntoni F (2013) Muscular dystrophies. *Lancet* **381**:845-860 https://doi.org/10.1016/s0140-6736(12)61897-2 | PubMed

Morton SM, Bastian AJ (2006) Cerebellar contributions to locomotor adaptations during splitbelt treadmill walking. *J Neurosci* **26**:9107-9116 https://doi.org/10.1523/jneurosci.2622-06.2006 | PubMed

Murata Y, Higo N, Oishi T, Yamashita A, Matsuda K, Hayashi M, Yamane S (2008) Effects of motor training on the recovery of manual dexterity after primary motor cortex lesion in macaque monkeys. *J Neurophysiol* **99**:773-786 https://doi.org/10.1152/jn.01001.2007 | PubMed

Mussa-Ivaldi FA, Bizzi E (1995) The Modular Organization of Motor Control: What Frogs Can Teach Us About Adaptive Learning. *IFAC Proceedings Volumes* **28**:413-418 https://doi.org/10.1016/s1474-6670(17)45267-0

Nakajima N, Wang S, Ogihara N, Oya T, Seki K, Funato T (2023) Upper Limb Musculoskeletal Model of Macaque Monkey for Approaching Adaptation Mechanism to Tendon Transfer. In: Neuroscience 2023 Abstracts. Washington, DC. Society for Neuroscience.

Nath T, Mathis A, Chen AC, Patel A, Bethge M, Mathis MW (2019) Using DeepLabCut for 3D markerless pose estimation across species and behaviors. *Nature Protocols* **14**:2152-2176 https://doi.org/10.1038/s41596-019-0176-0 | PubMed

Nordez A, Gallot T, Catheline S, Guével A, Cornu C, Hug F (2009) Electromechanical delay revisited using very high frame rate ultrasound. *J Appl Physiol (1985)* **106**:1970-1975 https://doi.org/10.1152/japplphysiol.00221.2009 | PubMed

Nudo RJ, Wise BM, SiFuentes F, Milliken GW (1996) Neural substrates for the effects of rehabilitative training on motor recovery after ischemic infarct. *Science* **272**:1791-1794 https://doi.org/10.1126/science.272.5269.1791 | PubMed

Osu R, Franklin DW, Kato H, Gomi H, Domen K, Yoshioka T, Kawato M (2002) Short- and long-term changes in joint co-contraction associated with motor learning as revealed from surface EMG. *J Neurophysiol* **88**:991-1004 https://doi.org/10.1152/jn.2002.88.2.991 | PubMed

Overduin SA, d'Avella A, Roh J, Bizzi E (2008) Modulation of Muscle Synergy Recruitment in Primate Grasping. *The Journal of Neuroscience* **28**:880-892 https://doi.org/10.1523/jneurosci.2869-07.2008 | PubMed

Petitet P, O'Reilly JX, O'Shea J (2018) Towards a neuro-computational account of prism adaptation. *Neuropsychologia* **115**:188-203 https://doi.org/10.1016/j.neuropsychologia.2017.12.021 | PubMed

Popa LS, Streng ML, Hewitt AL, Ebner TJ (2016) The Errors of Our Ways: Understanding Error Representations in Cerebellar-Dependent Motor Learning. *Cerebellum* **15**:93-103 https://doi.org/10.1007/s12311-015-0685-5 | PubMed

Power JD, Schlaggar BL (2017) Neural plasticity across the lifespan. *Wiley Interdiscip Rev Dev Biol* **6** https://doi.org/10.1002/wdev.216 | PubMed

Ranganathan R, Adewuyi A, Mussa-Ivaldi FA (2013) Learning to be lazy: exploiting redundancy in a novel task to minimize movement-related effort. *J Neurosci* **33**:2754-2760 https://doi.org/10.1523/jneurosci.1553-12.2013 | PubMed

Sattin D, Parma C, Lunetta C, Zulueta A, Lanzone J, Giani L, Vassallo M, Picozzi M, Parati EA (2023) An Overview of the Body Schema and Body Image: Theoretical Models, Methodological Settings and Pitfalls for Rehabilitation of Persons with Neurological Disorders. *Brain Sci* **13** https://doi.org/10.3390/brainsci13101410 | PubMed

Schärli A, Hecht H, Mast FW, Hossner EJ (2024) How spotting technique affects dizziness and postural stability after full-body rotations in dancers. *Hum Mov Sci* **95**:103211 https://doi.org/10.1016/j.humov.2024.103211 | PubMed

Schoultz TW, Swett JE (1972) The fine structure of the Golgi tendon organ. *J Neurocytol* **1**:1-26 https://doi.org/10.1007/bf01098642 | PubMed

Slawinska U, Kasicki S (2002) Altered Electromyographic Activity Pattern of Rat Soleus Muscle Transposed into the Bed of Antagonist Muscle. *The Journal of Neuroscience* **22**:5808 https://doi.org/10.1523/JNEUROSCI.22-14-05808.2002 | PubMed

Smith MA, Shadmehr R (2005) Intact ability to learn internal models of arm dynamics in Huntington's disease but not cerebellar degeneration. *J Neurophysiol* **93**:2809-2821 https://doi.org/10.1152/jn.00943.2004 | PubMed

Smith MA, Ghazizadeh A, Shadmehr R (2006a) Interacting Adaptive Processes with Different Timescales Underlie Short-Term Motor Learning. *PLOS Biology* **4**:e179 https://doi.org/10.1371/journal.pbio.0040179 | PubMed

Smith MA, Ghazizadeh A, Shadmehr R (2006b) Interacting adaptive processes with different timescales underlie short-term motor learning. *PLoS Biol* **4**:e179 https://doi.org/10.1371/journal.pbio.0040179 | PubMed

Smith SA, Mitchell JH, Garry MG (2006c) The mammalian exercise pressor reflex in health and disease. *Exp Physiol* **91**:89-102 https://doi.org/10.1113/expphysiol.2005.032367 | PubMed

Sperry RW (1940) The functional results of muscle transposition in the hind limb of the rat. *Journal of Comparative Neurology* **73**:379-404 https://doi.org/10.1002/cne.900730303

Sperry RW (1942) Transplantation of motor nerves and muscles in the forelimb of the rat. *Journal of Comparative Neurology* **76** https://doi.org/10.1002/cne.900760206

Sperry RW (1947) Effect of crossing nerves to antagonistic limb muscles in the monkey. *Arch Neurol Psychiatry* **58**:452-473 https://doi.org/10.1001/archneurpsyc.1947.02300330064006 | PubMed

Sugita Y (1996) Global plasticity in adult visual cortex following reversal of visual input. *Nature* **380**:523-526 https://doi.org/10.1038/380523a0 | PubMed

Takei T, Seki K (2010) Spinal interneurons facilitate coactivation of hand muscles during a precision grip task in monkeys. *J Neurosci* **30**:17041-17050 https://doi.org/10.1523/jneurosci.4297-10.2010 | PubMed

Takei T, Confais J, Tomatsu S, Oya T, Seki K (2017) Neural basis for hand muscle synergies in the primate spinal cord. *Proceedings of the National Academy of Sciences* **114**:8643-8648 https://doi.org/10.1073/pnas.1704328114 | PubMed

Takeuchi N, Izumi S (2012) Maladaptive plasticity for motor recovery after stroke: mechanisms and approaches. *Neural Plast* **2012**:359728 https://doi.org/10.1155/2012/359728 | PubMed

Tannenbaum J, Bennett BT (2015) Russell and Burch's 3Rs then and now: the need for clarity in definition and purpose. *J Am Assoc Lab Anim Sci* **54**:120-132 PubMed

Thompson AK, Wolpaw JR (2014) Operant conditioning of spinal reflexes: from basic science to clinical therapy. *Front Integr Neurosci* **8**:25 https://doi.org/10.3389/fnint.2014.00025 | PubMed

Thoroughman KA, Shadmehr R (1999) Electromyographic correlates of learning an internal model of reaching movements. *J Neurosci* **19**:8573-8588 https://doi.org/10.1523/jneurosci.19-19-08573.1999 | PubMed

Trewartha KM, Garcia A, Wolpert DM, Flanagan JR (2014) Fast but fleeting: adaptive motor learning processes associated with aging and cognitive decline. *J Neurosci* **34**:13411-13421 https://doi.org/10.1523/jneurosci.1489-14.2014 | PubMed

Valero-Cuevas FJ, Hentz VR (2002) Releasing the A3 pulley and leaving flexor superficialis intact increases pinch force following the Zancolli lasso procedures to prevent claw deformity in the intrinsic palsied finger. *J Orthop Res* **20**:902-909 https://doi.org/10.1016/s0736-0266(02)00040-2 | PubMed

Vallbo AB, Hagbarth KE, Torebjörk HE, Wallin BG (1979) Somatosensory, proprioceptive, and sympathetic activity in human peripheral nerves. *Physiol Rev* **59**:919-957 https://doi.org/10.1152/physrev.1979.59.4.919 | PubMed

van Vliet P, Carey LM, Turton A, Kwakkel G, Palazzi K, Oldmeadow C, Searles A, Lavis H, Middleton S, Galloway M, *et al.* (2023) Task-specific training versus usual care to improve upper limb function after stroke: the "Task-AT Home" randomised controlled trial protocol. *Frontiers in Neurology* **14** https://doi.org/10.3389/fneur.2023.1140017 | PubMed

Vanhoof MJM, van Leeuwen T, Galletta L, Vereecke EE (2021) The forearm and hand musculature of semi-terrestrial rhesus macaques (Macaca mulatta) and arboreal gibbons (fam. Hylobatidae). Part II. Quantitative analysis. *Journal of Anatomy* **238**:321-337 https://doi.org/10.1111/joa.13314 | PubMed

Villalta JI, Landi SM, Fló A, Della-Maggiore V (2013) Extinction Interferes with the Retrieval of Visuomotor Memories Through a Mechanism Involving the Sensorimotor Cortex. *Cerebral Cortex* **25**:1535-1543 https://doi.org/10.1093/cercor/bht346 | PubMed

Walker JG, Jackson HJ, Littlejohn GO (2004) Models of adjustment to chronic illness: using the example of rheumatoid arthritis. *Clin Psychol Rev* **24**:461-488 https://doi.org/10.1016/j.cpr.2004.03.001 | PubMed

Wester K, Hove LM, Barndon R, Craven AR, Hugdahl K (2018) Cortical Plasticity After Surgical Tendon Transfer in Tetraplegics. *Front Hum Neurosci* **12**:234 https://doi.org/10.3389/fnhum.2018.00234 | PubMed

Winterbottom L, Nilsen DM (2024) Motor Learning Following Stroke: Mechanisms of Learning and Techniques to Augment Neuroplasticity. *Phys Med Rehabil Clin N Am* **35**:277-291 https://doi.org/10.1016/j.pmr.2023.06.004 | PubMed

Wolpert DM (1997) Computational approaches to motor control. *Trends Cogn Sci* **1**:209-216 https://doi.org/10.1016/s1364-6613(97)01070-x | PubMed

Yan Y, Sobinov AR, Bensmaia SJ (2022) Prehension kinematics in humans and macaques. *J Neurophysiol* **127**:1669-1678 https://doi.org/10.1152/jn.00522.2021 | PubMed

Yumiya H, Larsen KD, Asanuma H (1979) Motor readjustment and input-output relationship of motor cortex following cross-connection of forearm muscles in cats. *Brain Research* **177**:566-570 https://doi.org/10.1016/0006-8993(79)90474-8 | PubMed

Zajac FE (1992) How musculotendon architecture and joint geometry affect the capacity of muscles to move and exert force on objects: a review with application to arm and forearm tendon transfer design. *J Hand Surg Am* **17**:799-804 https://doi.org/10.1016/0363-5023(92)90445-u | PubMed

Zeiler SR, Krakauer JW (2013) The interaction between training and plasticity in the poststroke brain. *Curr Opin Neurol* **26**:609-616 https://doi.org/10.1097/wco.0000000000000025 | PubMed

Zemková E (2022) Physiological Mechanisms of Exercise and Its Effects on Postural Sway: Does Sport Make a Difference?. *Front Physiol* **13**:792875 https://doi.org/10.3389/fphys.2022.792875 | PubMed

Peer reviews

Reviewer #1 (Public review):

Summary:

Many studies have investigated adaptation to altered sensorimotor mappings or to an altered mechanical environment. This paper asks a different but also important question in motor control and neurorehabilitation: how does the brain adapt to changes in the controlled plant? The authors addressed this question by performing a tendon transfer surgery in two monkeys during which the swapped tendons flexing and extending the digits. They then monitored changes in task performance, muscle activation and kinematics post-recovery over several months, to assess changes in putative neural strategies.

Strengths:

(1) The authors performed complicated tendon transfer experiments to address their question of how the nervous system adapts to changes in the organisation of the neuromusculoskeletal system, and present very interesting data characterising neural (and in one monkey, also behavioural) changes post tendon transfer over several months.

(2) The fact that the authors had to employ to two slightly different tasks -one more artificial, the other more naturalistic- in the two monkeys and yet found qualitatively similar changes across them makes the findings more compelling. After all these are very challenging experiments!

(3) The paper is well written, the analyses are sound, and the authors interpret the data appropriately, acknowledging the key limitations.

Weaknesses:

None of note.

https://doi.org/10.7554/eLife.108684.2.sa2

Reviewer #3 (Public review):

Summary:

In this study, Philipp et al. investigate how a monkey learns to compensate for a large, chronic biomechanical perturbation--a tendon transfer surgery, swapping the actions of two muscles that flex and extend the fingers. After performing the surgery and confirming that the muscle actions are swapped, the authors follow the monkeys' performance on grasping tasks over several months. There are several main findings:

- There is an initial stage of learning (around 60 days), where monkeys simply swap the activation timing of their flexors and extensors during the grasp task to compensate for the two swapped muscles.

- This is (seemingly paradoxically) followed by a stage where muscle activation timing returns almost to what it was pre-surgery, suggesting that monkeys suddenly swap to a new strategy that is better than the simple swap.

- Muscle synergies seem remarkably stable through the entire learning course, indicating that monkeys do not fractionate their muscle control to swap the activations of only the two transferred muscles.

- Muscle synergy activation shows a similar learning course, where the flexion synergy and extension synergy activations are temporarily swapped in the first learning stage and then revert to pre-surgery timing in the second learning stage.

- The second phase of learning seems to arise from making new, compensatory movements (supported by other muscle synergies) that get around the problem of swapped tendons.

Strengths:

This study is quite remarkable in scope, studying two monkeys over a period of months after a difficult tendon-transfer surgery. As the authors point out, this kind of perturbation is an excellent testbed for the kind of long-term learning that one might observe in a patient after stroke or injury, and provides unique benefits over more temporary perturbations like visuomotor transformations and over studying learning through development. Moreover, while the two-stage learning course makes sense, I found the details to be genuinely surprising--specifically the fact that: 1) muscle synergies continue to be stable for months after the surgery, despite being maladaptive; and 2) muscle activation timing reverts to pre-surgery levels by the end of the learning course. These two facts together initially make it seem like the monkey simply ignores the new biomechanics by the end of the learning course, but the authors do well to explain that this is mainly because the monkeys develop a new kind of movement to circumvent the surgical manipulation.

I found these results fascinating, especially in comparison to some recent work in motor cortex, showing that a monkey may be able to break correlations between the activities of motor cortical neurons, but only after several of coaching and training (Oby et al. PNAS 2019). Even then, it seemed like the monkey was not fully breaking correlations but rather pushing existing correlations harder to get succeed at the virtual task (a brain-computer interface with perturbed control).

Weaknesses:

I found the analysis to be reasonably well considered and relatively thorough. The authors have also suitably addressed my comments on the previous version. One minor weakness that remains (understandably so) is that the two animals in the study performed different tasks, and the results of the secondary synergy analysis seem to be quite different (Figure 10).

That said, I don't think this weakness reduces the impact of the study, and though multiple replications of the same results would provide more convincing evidence, I don't think it's necessary to make the points that the authors are making.

https://doi.org/10.7554/eLife.108684.2.sa1

Author response:

The following is the authors' response to the original reviews.

> ***Public Reviews:***
>
> ***Reviewer #1 (Public review):***
>
> *(1) I think this is an important paper, but I'm puzzled about a tension in the results. On the one hand, it looks like the behavioural gains post-TT happen rather smoothly over time (Figure 5). On the other hand, muscle synergy activations change abruptly at specific days (around day ~65 for Monkey A and around day ~45 for Monkey B; e.g., Figure 6). How do the authors reconcile this tension? In other words, how do they think that this drastic behavioural transition can arise from what appears to be step-by-step, continuous changes in muscle coordination? Is it "just" subtle changes in movements/posture exploiting the mechanical coupling between wrist and finger movements, combined with subtle changes in synergies, and they just happen to all kick in at the same time? This feels to me to be the core of the paper and should be addressed more directly.*

We thank the reviewer for this insightful comment, as it touches upon the central finding of our study. The apparent tension between the smooth behavioral recovery and the abrupt shift in neural strategy is indeed a key feature of the adaptation process. We propose that this reflects the interaction of two distinct, parallel processes operating on different timescales:

A slow, gradual skill-learning process, where the monkeys incrementally developed and refined a compensatory motor strategy (i.e., the tenodesis effect). This slow refinement is responsible for the smooth improvement seen in the behavioral metrics over many weeks.

A fast, switch-like adaptive process, which governs the activation of the primary muscle synergies. The initial 'swap' strategy, while simple, was biomechanically conflicting and inefficient. The CNS only abandoned this flawed strategy abruptly once the slow learning process had rendered the new compensatory strategy "good enough" to be a viable alternative.

Therefore, the abrupt neural shift does not cause the behavioral improvement but is rather enabled by the gradual, underlying development of a better motor solution. To address this important point more directly within the manuscript, we added a new subheading to the Discussion section. This section is dedicated to explicitly framing our findings within this multi-timescale learning model, ensuring the link between the gradual behavioral recovery and the abrupt neural shift is clearly articulated.

> *(2) The muscle synergy analyses, which are an important part of the paper, could be improved. In particular:*
>
> *(a) When measuring the cross-correlation between the activation of synergies, the authors should include error bars and should also look at the lag between the signals.*

We thank the reviewer for these excellent suggestions to improve our analysis.

Error Bars: We agree that showing trial-to-trial variability is important. In our revision, we have added a shaded envelope (representing the SD across trials) to the cross-correlation

plots in Figures 6, 9 and 10.

Time Lag: We have performed the cross-correlation analysis allowing for variable time lags and extracted the lag yielding the maximum correlation coefficient (max CC) for each session, in addition to the zero-lag correlation presented in the main figures. As hypothesized, allowing variable lags often resulted in high max CC values throughout the adaptation period, potentially obscuring the clear swap-and-revert pattern visible in the zerolag analysis. This is likely because the primary adaptation involved changes in synergy timing rather than fundamental shape. However, the analysis of the lag itself proved informative. We observed significant fluctuations in the optimal lag during the early and mid-adaptation phases, particularly around the time of the 'switch-back', before the lag stabilized closer to zero in the late phase.

We have added a description of this analysis to the Methods section. The results of the lag analysis are now presented in a new Supplementary Figure S6 and S7, and a sentence summarizing this finding has been added to the Results section.

> *(b) Figure 7C and related figures, the authors state that the activation of muscle synergies reverts to pre-TT patterns toward the end of the experiments. However, there are noticeable differences for both monkeys (at the end of the "task range" for synergy B for monkey A, and around 50% task range for synergy B for monkey B). The authors should measure this, e.g., by quantifying the per-sample correlation between pre-TT and post-TT activation amplitudes. Same for Figures 8I, J, etc.*

We thank the reviewer for this detailed and insightful suggestion. We agree that our use of the term 'reversion' should be nuanced, as the recovery of the synergy activation patterns is substantial but not perfect.

To formally quantify these remaining differences, we performed a rigorous quantitative comparison between the pre-surgery and final-day post-surgery activation profiles. We calculated the Cosine Similarity to assess the recovery of the temporal shape, and used a Permutation Test (n=10,000) to test for statistical distinctness between the pre- and post-surgery trajectories.

Results: We found that while the temporal shapes were highly similar (Cosine Correlation > 0.90 for all synergies), the Permutation Test confirmed that the profiles remained statistically distinct ($p < 0.0001$) in both animals.

We have added this quantification to the text (Results). This confirms our nuanced interpretation: while the primary temporal features of the synergies reverted, the recovered motor program represents a novel, 'good enough' solution that is robust and functional, rather than a mathematically perfect restoration of the original baseline.

> *(c) In Figures 9 and 10, the authors show the cross-correlation of the activation coefficients of different synergies; the authors should also look at the correlation between activation profiles because it provides additional information.*

We thank the reviewer for this comment and the opportunity to clarify our terminology. We agree that analyzing the correlation between the full activation profiles is the most informative approach. In our manuscript, the terms 'activation coefficients' and 'activation profiles' both refer to the complete, time-varying activation patterns of the muscle synergies. Therefore, the crosscorrelation analysis presented in Figures 9 and 10 is indeed the correlation between these full activation profiles. To prevent any potential ambiguity for future readers, we have revised the manuscript to use the term 'activation profiles' exclusively and consistently when referring to these time-varying synergy activations.

> *(d) The muscle synergy analysis for Monkey B is hindered by the fact that the authors lost the ability to record from the (very) functionally relevant FDS muscle. I'd repeat the synergy analyses without this muscle to understand to what extent the observed changes with respect to baseline are driven by the lack of this data.*

We thank the reviewer for raising this important methodological point. We agree that controlling for changes in the recorded muscle set is crucial for a valid comparison between pre- and post-surgical synergy structures. The reviewer's concern is based on the premise that the FDS muscle was included in the pre-surgical analysis for Monkey B but absent from the postsurgical analysis.

We would like to clarify that this is not the case. Due to the loss of the FDS signal post-surgery, we made the deliberate decision to exclude the FDS muscle from ALL synergy analyses for Monkey B, including the pre-surgical baseline period. This was done for the precise reason the reviewer identifies: to ensure a direct and unbiased "apples-to-apples" comparison and to avoid introducing the lack of this muscle as a confound. Therefore, the changes in synergy structure that we report for Monkey B can be confidently attributed to genuine physiological adaptation rather than an artifact of a changing input dataset.

> *(e) Figure 11: The authors talk about a key difference in how Synergy B (the extensor finger) evolved between monkeys post-TT. However, to me this figure feels more like a difference in quantity - the time course than quality, since for both monkeys the aaEMG levels pretty much go back to close to baseline levels - even if there's a statistically significant difference only for Monkey B. What am I missing?*

We thank the reviewer for this insightful question, as it has prompted us to refine our interpretation of this key finding. The reviewer correctly notes that the recovery trajectories of Synergy B appear different, and we agree that our original explanation can be improved.

A more parsimonious interpretation, and one that we believe aligns better with the data, is that both monkeys likely underwent a similar 'arms race', but we captured different phases of this process. In Monkey A, our recordings (starting Day 29) captured the escalating phase of this neuromuscular conflict. In contrast, for Monkey B, recordings began on Day 20, by which time this rapid escalation had likely already occurred and peaked. This difference in the timing of the 'arms race' is consistent with our behavioral observations; Monkey A struggled for a longer period before performing the task proficiently, suggesting a more protracted overall adaptation process. Thus, the apparent difference in the figures is likely a reflection of the observational window and the individual adaptation rate of each animal, rather than a fundamental qualitative difference in their adaptive strategy. We have revised the text to present this more unified and coherent interpretation.

> *(f) Lines 408-09 and above: The authors claim that "The development of a compensatory strategy, primarily involving the wrist flexor synergy (Synergy C), appears crucial for enabling the final phase of adaptation", which feels true intuitively and also based on the analysis in Figure 8, but Figure 11 suggests this is only true for Monkey B. How can these statements be reconciled?*

We believe the reviewer may be referring to Monkey A in their comment, as the strong compensatory effect is indeed seen in this animal. The core of this issue, which we have clarified in our revision, is that both monkeys developed a compensatory tenodesis grasp but used different neural strategies to achieve it.

For Monkey A, strong evidence for this strategy is provided by a clear temporal shift in the activation of its dedicated wrist flexor synergy (Synergy C). As we have now clarified in the manuscript, the peak of this synergy's activation moved from occurring just after object contact to just before it, a re-timing well-suited to enable a tenodesis grasp.

For Monkey B, the strategy was one of subtle re-timing rather than scaling. While the total aggregated activation of its primary flexor synergy (Synergy A) did not significantly increase, its temporal profile shifted. Specifically, activation prior to object contact increased, providing the necessary wrist flexion for its assistive tenodesis grasp, which was kinematically confirmed in Figure 12. This was achieved by reallocating activation from the post-contact phase, resulting in an earlier activation peak for the synergy overall. Crucially, a finer-grained analysis reveals a precise temporal sequence within this synergy's activation: the wrist flexor component (PL) consistently peaked just before object contact to enable hand opening, while the finger flexor component (FDP) peaked just after contact to secure the grasp.

This timing resolves the apparent biomechanical conflict. It also reveals that while both monkeys converged on the same biomechanical solution (a tenodesis grasp), the observable neural implementation appeared different. However, we must be cautious in directly comparing the computed synergy structures themselves, as the analysis for Monkey B was performed without the FDS muscle. The apparent "multi-functional synergy" in Monkey B is most likely a consequence of this missing data. What is clear and robust, however, is that both monkeys converged on a remarkably similar temporal solution: they both learned to re-time the activation of their key wrist flexor muscles to the pre-grasp phase.

In Monkey A, this was observed in the temporal shift of its dedicated wrist flexor synergy (Synergy C). In Monkey B, this was observed in the temporal shift of the Palmaris Longus (PL) muscle itself (which, in our computed synergies, was grouped into Synergy A). This convergence on an identical temporal adaptation, regardless of the computed modular organization, is the key finding. We have revised the manuscript to articulate this more precise and defensible interpretation.

> *(3) Experimental design: at least for the monkey who was trained on the "artificial task" (Monkey A), it would have been good if the authors had also tested him on naturalistic grasping, like the second monkey, to see to what extent the neural changes generalise across behaviours or are task-specific. Do the authors have some data that could be used to assess this even if less systematically?*

We thank the reviewer for raising this important point regarding the generalizability of our findings across different behaviors. We fully agree that a direct comparison of both tasks in the same animal would have been a valuable experiment. Unfortunately, we do not have systematic data on naturalistic grasping for Monkey A that would allow for such a direct comparison. We therefore view the two tasks as providing complementary evidence. Monkey A's data shows the adaptation process during a highly stereotyped behavior, while Monkey B's data demonstrates that a similar two-phase adaptive process occurs during a more naturalistic, unconstrained task. The convergence of these findings strengthens our overall conclusion that this multi-timescale adaptation is a robust principle of motor learning. Nonetheless, the reviewer raises a fascinating question about the task-specific tuning of motor synergies, which remains an excellent direction for future studies.

> *(4) Monkey B's behaviour pre-tendon transfer seems more variable than that of Monkey A (e.g., the larger error bars in Figure 5 compared to monkey A, the fluctuating crosscorrelation between FDS pre and EDC post in Figure 6Q). This should be quantified to better ground the results since it also shows more variability post-TT.*

We thank the reviewer for this excellent suggestion to formally quantify the presurgery behavioral variability. We have performed the suggested analysis on the "Grip Formation Time" metric (Fig. 5A), which was the comparable metric between the two tasks. Our calculation of the Coefficient of Variation (CV) confirms the reviewer's observation. Monkey B's pre-surgery performance was substantially more variable (CV = 81.93%) than Monkey A's

(CV = 46.62%). Furthermore, a non-parametric test for equal variances (Ansari-Bradley test) confirmed that this difference is highly statistically significant ($p < 0.0001$). We have added a description of this analysis to the Methods and reported this finding in the Results section to provide a clearer context for the baseline differences between the subjects.

> *(5) Minor: Figure 12 is interesting and supports the idea that monkeys may exploit the biomechanical coupling between wrist and fingers as part of their functional recovery. It would be interesting to measure whether there is a change in such coupling (tenodesis) over time, e.g., by plotting the change in wrist angle vs change in MCP angle as a scatter plot (one dot per trial), and in the same plot show all the days, colour coded by day. Would the relationship remain largely constant or fluctuate slightly early on? I feel this analysis could also help address my point (1) above.*

We thank the reviewer for this excellent and insightful suggestion. We have performed the suggested analysis for Monkey B, plotting the trial-by-trial relationship between wrist and MCP angles for all recording days (New Figure 13).

The results clearly show the gradual refinement of the tenodesis coupling. Pre-surgery, there was no correlation (R^2=0.00). Immediately post-surgery (Day 22), the relationship was weak and variable (R^2=0.16), reflecting an exploratory phase. Over the following weeks, the coupling became progressively stronger and more consistent, with the R^2 value peaking at 0.58 around Day 56, indicating a robust exploitation of the new strategy. The relationship then stabilized at a moderate level (R^2 ~0.2-0.3) in the final days. This analysis provides direct kinematic evidence for the slow, gradual skill-learning component of our two-state model. It beautifully complements our response to the reviewer's first point by visualizing the underlying refinement process that occurred concurrently with the more abrupt neural shifts. We have added this new figure and a description of these results to the manuscript.

> ***Reviewer #2 (Public review):***
>
> *Weaknesses:*
>
> *The most notable weakness of the study is the incompleteness of the data. […] As a result, it is difficult to make general conclusions from the study, and it awaits further analysis or the addition of another subject.*

We thank the reviewer for this critical and accurate assessment of the study's limitations. The reviewer is correct that the datasets for the two monkeys are incomplete in different ways and that the tasks were not identical. We fully acknowledge these limitations throughout the manuscript. Rather than viewing these differences as a weakness that prevents generalization, we propose that they offer a unique strength in the form of complementary evidence. We consider the two animals not as a direct replication, but as two distinct case studies that test the same underlying hypothesis under different conditions.

Monkey A, with its high-quality EMG and highly stereotyped task, provides a detailed, quantitative view of the neural adaptation process, allowing us to precisely characterize phenomena like the 'neuromuscular arms race'.

Monkey B, with its kinematic data and more naturalistic task, provides crucial evidence that the same fundamental principles, a two-phase adaptation and the eventual development of a compensatory strategy, generalize to a less constrained, more behaviorally relevant context. We believe the key finding is the convergence of the results. Despite the differences in individual strategy, task demands, and available data, both animals demonstrated the same core "swapand-revert" adaptive process. We propose that this convergence from heterogeneous sources lends support to the generalizability of our conclusions, suggesting that the multi-timescale adaptation we describe may be a general feature of motor learning following such perturbations. We agree that future studies with more subjects are needed to

fully establish this principle. Nonetheless, we feel that the convergent evidence from these two complementary cases provides a valuable foundation for the model we present.

> *A second weakness is the insufficient analysis of the movements themselves, particularly for Monkey A. [...] Since the authors have video data for both monkeys, it is surprising that it was not used to extract landmarks for kinematic analysis, or at least hand/endpoint trajectory, and how it is adjusted over time. Adding more behavior data and aligning it with the EMG data would be very helpful for characterizing motor recovery and is needed to support conclusions about underlying neural control strategies for functional improvement.*

We thank the reviewer for this important suggestion. The reviewer's comment prompted us to re-examine our behavioral data, and we have now performed additional analyses that we agree provide a much clearer link between the neural changes and functional recovery.

For Monkey A, we have quantified the 'pull times' on a day-by-day basis. This analysis reveals a clear, gradual learning curve: pull times were initially long and variable post-surgery but steadily decreased and stabilized over the recovery period. This provides a direct, quantitative measure of motor performance recovery for this animal.

For Monkey B, we have performed a detailed analysis of the 'grasp aperture' prior to object contact. This kinematic analysis is particularly revealing, as it shows the development of the compensatory strategy in real-time. The grasp aperture was initially very small post-surgery, reflecting the monkey's inability to open its hand. It then steadily increased over the next ~40 days as the monkey learned and refined the compensatory tenodesis grasp, before stabilizing at a new, functional baseline.

We believe these new analyses directly address the reviewer's concern by providing a more detailed picture of motor recovery. The grasp aperture data, in particular, offers a clear kinematic correlate for the slow, skill-learning process that we propose runs in parallel to the more abrupt neural reorganization. We have added these results as a new figure in the main text of our revised manuscript.

> *Considering specific conclusions, the statement that the monkeys learned to use "tenodesis" over time by increasing activation of a wrist flexor muscle synergy does not seem to be fully supported by the data. [...] Given these issues, it is not clear how to align the EMG and kinematic data and interpret these findings.*

We thank the reviewer for this detailed and critical analysis. They raise an excellent point and have correctly observed that the adaptation is not a simple, uniform increase in wrist flexor synergy amplitude. Our interpretation, which we have clarified in the manuscript, is that the monkeys learned a more sophisticated strategy: a precise re-timing of the wrist flexor activation to occur earlier in the movement, specifically to pre-shape the hand for the grasp.

For Monkey A: The reviewer correctly notes that the peak amplitude of Synergy C (the wrist flexor synergy) around the moment of grasp (0% task range) is lower in the final phase compared to baseline. However, the crucial change is temporal: the peak of this synergy's activation shifts from occurring just after the grasp (~+1%) to occurring just before it (~-2%). This re-timing is perfectly suited to enable finger extension via the tenodesis effect immediately prior to object contact. The subsequent lower amplitude may reflect a more efficient, less forceful movement once this new skill was refined.

For Monkey B: The reviewer is right that this monkey does not have a dedicated wrist flexor synergy and that the overall amplitude of the PL muscle does not increase dramatically. However, a closer look at its activity profile (Fig. S2-AN) reveals a clear and consistent increase in activation specifically in the pre-contact phase (~7% task range). This is the precise neural signature of the assistive tenodesis grasp that is kinematically confirmed in

Figure 12. The monkey is not simply scaling up the synergy; it is strategically activating it earlier to prepare for the grasp.

In summary, the key evidence linking the EMG to the tenodesis strategy is in the temporal domain. The learned re-timing of the wrist flexor activation to the pre-grasp phase is the crucial link that aligns the neural and kinematic data. We have revised the manuscript to make this distinction between amplitude scaling and temporal shifting clearer.

> *A more minor point regarding conclusions: statements about poor task performance and high energy expenditure being the costs that drive exploration for a new strategy are speculative and should be presented as such. Although the monkeys did take longer to complete the tasks after the surgery, they were still able to perform it successfully and in less than a second and no measurements of energy expenditure were taken.*

We thank the reviewer for this important point regarding the precision of our language. We agree that statements regarding 'high energy expenditure' and the specific drivers for exploring a new strategy are interpretations of the data, not direct measurements, and should be framed as such.

Our speculation about energetic cost is based on the significant increase in muscle co-activation we observed (e.g., Fig. 11), a phenomenon widely understood to be metabolically expensive. Similarly, while the monkeys were still successful, their prolonged movement times and inefficient motor patterns represent a clear performance deficit compared to their highly optimized presurgical baseline, which we propose acted as a driver for further adaptation. In our full revision, we have carefully revised the manuscript to soften these claims. We have used more speculative language, such as "we hypothesize that...", "the likely cost of...", or "may have provided the impetus for..." to ensure that our interpretations are clearly distinguished from our direct empirical findings.

> *A small concern is whether the tendon transfer effect may fail over time, either due to scar tissue formation or tendon tearing, and it would be ideal if the integrity of the intervention were re-assessed at the end of the study.*

We thank the reviewer for raising this important point regarding the long-term integrity of the tendon transfer. We agree that a terminal anatomical re-assessment would be an ideal control. While a terminal assessment was not performed as part of this study's protocol, we were able to monitor the transfer's integrity throughout the study. We are confident the transfer remained functionally intact for two key reasons:

(1) Physical Monitoring: We periodically used ultrasound imaging to non-invasively visualize the tendon repair, which allowed us to confirm its continued physical integrity.

(2) Functional Evidence: This physical confirmation was corroborated by the functional data. Both animals achieved stable, proficient task performance that was maintained for months. Furthermore, the late-phase neuromuscular control strategies became highly consistent. A significant failure, such as a tendon tear or prohibitive mechanical scarring, would be incompatible with this sustained behavioral and neural stability.

Nevertheless, we agree that a terminal assessment is an excellent methodological suggestion that should be incorporated into the design of future long-term studies of this nature.

> ***Reviewer #3 (Public review):***
>
> *(1) First, I find myself wondering about the physical healing process from the tendon transfer surgery and how it might contribute to the learning. Specifically, how long does it take for the tendons to heal and bear forces? If this itself takes a few months, it would be nice to see some discussion of this.*

We thank the reviewer for this insightful question about the potential contribution of the physical healing process to the adaptation timeline. Our surgical protocol was specifically designed to ensure the tendon transfer was biomechanically robust from the outset, minimizing the role of healing as a rate-limiting factor.

We used a Pulvertaft weave technique, which is known to achieve mechanical strength equivalent to that of a native tendon shortly after the procedure (Graham et al., 2023). The repair involved more than two weaves and utilized high-strength suture material to maximize its initial forcebearing capacity. While full fibrous integration around the suture site typically occurs within approximately six weeks, the repair itself was strong enough to bear physiological forces immediately post-surgery. Therefore, the prolonged, complex, two-phase multi-month behavioral recovery and the neural reorganization we observed cannot be attributed to a slow physical healing process. Instead, this supports our conclusion that the observed timeline reflects the challenges and constraints of a purely neural adaptation and skill-learning process. To make this crucial point clear to all readers, we have added these details about the surgical method to the Methods section and included a brief discussion of its implications in the Discussion.

> *(2) Second, I see that there are some changes in the muscle loadings for each synergy over the days, though they are relatively small. The authors mention that the cosine distances are very small for the conserved synergies compared to distances across synergies, but it would be good to get a sense for how variable this measure is within synergy. For example, what is the cosine similarity for a conserved synergy across different pre-surgery days? This might help inform whether the changes post-surgery are within a normal variation or whether they reflect important changes in how the muscles are being used over time.*

We thank the reviewer for this excellent and insightful suggestion. Establishing a baseline for normal day-to-day variability is an important control for our synergy analysis.

We have performed this analysis in full. Specifically, to quantify baseline stability, we calculated the cosine similarity between the spatial synergy weights (W) of each individual recording day and the pre-surgery average. This provides a rigorous measure of day-to-day variability relative to the stable baseline structure. We have added these data to Figure 7 (Panel I), which plots the pre-surgery similarity (blue traces) alongside the post-surgery adaptation (red traces).

We found that baseline stability was remarkably high, with cosine similarity consistently exceeding 0.99 (e.g., Monkey A: 0.99 ± 0.001). This quantification allows the reader to formally assess that the changes observed post-surgery (e.g., drops to ~0.80 or ~0.60 in Monkey B) are well outside the range of normal physiological fluctuation, representing subtle but genuine structural adaptation.

> *(3) Last, and maybe most difficult (and possibly out of scope for this work): I would have ideally liked to see some theoretical modeling of the biomechanics so I could more easily understand what the tendon transfer did or how specific synergies affect hand kinematics before and after the surgery. Especially given that the synergies remained consistent, such an analysis could be highly instructive for a reader or to suggest future perturbations to further probe the effects of tendon transfer on long-term learning.*

We thank the reviewer for this excellent and forward-thinking suggestion. We completely agree that a detailed biomechanical model of the tendon transfer would be a powerful tool for understanding the mechanical consequences of the surgery and for interpreting the function of the recorded muscle synergies. However, creating a subject-specific musculoskeletal model with the fidelity required to accurately simulate synergy-to-kinematic

transformations is a highly complex project that we feel is well beyond the scope of the current manuscript. Such an endeavor would constitute a major research project in its own right.

Our study's primary focus was to provide a detailed, longitudinal characterization of the in-vivo neural adaptation following this perturbation, a dataset that is itself rare and valuable. We aimed to document the physiological learning process as it unfolded over many months. Nonetheless, the reviewer's point is exceptionally well-taken. Currently, we are constructing a monkey musculoskeletal model and performing tendon transfer on this model to investigate what kind of characteristics in the learning process reproduce the synergy changes observed in the experiments. Although this project is still in progress, to date, we have demonstrated that the robustness of synergies themselves is necessary for changes in muscle activity at the synergy level (Nakajima N, Wang S, Ogihara N, Oya T, Seki K, Funato T, Upper Limb Musculoskeletal Model of Macaque Monkey for Approaching Adaptation Mechanism to Tendon Transfer, Society for Neuroscience 2023, Washington DC, USA, 2023).

The rich dataset we have collected in the present research could serve as an excellent foundation for developing and validating such a model in the future. We believe that combining these two approaches is a critical and exciting next step for the field, and we have highlighted this as a key future direction in our discussion.

> ***Recommendations for the authors:***
>
> ***Reviewing Editor Comments:***
>
> *When revising the manuscript for resubmission, please try to improve the visual presentation of the data, which is a point highlighted by all three reviewers during the discussion, including making the presentation of monkey-specific results more consistent across subjects.*

We have comprehensively revised the figures to ensure a consistent and clear visual presentation, as requested. Specifically, we standardized the layout across all main and supplementary figures (placing Monkey A consistently in the top rows or left columns and Monkey B in the bottom rows or right columns) and applied unified color schemes throughout the manuscript. Furthermore, we harmonized the presentation of the analytical results, such as the specific cross-correlation pairings in Figures 9 and 10, to ensure that the data for both subjects are presented with identical logic, facilitating direct comparison.

> ***Reviewer #1 (Recommendations for the authors):***
>
> *(1) Please revise the writing; some words are missing (line 90), and some sentences could be clarified slightly, even if the paper is well written (lines 317-320). The paragraph including the idea of tenodesis could also be further clarified, I think.*

Thank you for pointing these out. We have corrected the missing word (osteoarthritis) on line 90. We have also revised lines 317-320 to remove ambiguity. Furthermore, the section describing the tenodesis effect (now section "Distinct neural implementations...") has been substantially rewritten for improved clarity, incorporating a more detailed explanation of the biomechanics.

> *(2) In the Introduction, the authors cite Hunter and Eckstein 2009 and Mercuri and Muntoni 2013 without describing the pathological conditions; this will not be clear for not nonspecialists.*

Thank you. We have added brief descriptions ("osteoarthritis, a degenerative joint disease," and "muscular dystrophy, which involves progressive muscle weakness,") directly into the Introduction sentence where these references appear.

> *(3) Data presentation: I often thought that the data could be presented more clearly:*
>
> *(a) For example, Figure 3D and 4D should show error bars around the mean to have a sense of the consistency of pre-lesion behaviour. Same for other figures like Figure 6.*

We appreciate the reviewer's suggestion to visualize data consistency. (a) Figures 3D, 4D, and 6 (EMG Profiles): For these figures, we opted to display mean traces and peak markers to clearly illustrate the temporal shifts and relationships between muscles. Overlaying multiple standard deviation envelopes in these comparative plots would significantly reduce legibility. However, to fully address the reviewer's request to see the consistency of pre-lesion behavior, we direct attention to Supplementary Figure S1, which presents the complete EMG profiles with full error tubes (Mean ± SD) for every recorded muscle. (b) Quantitative Analysis Figures: We ensured that variability is explicitly visualized in all statistical analyses. The crosscorrelation time-courses in Figures 6 (G-Q), 9, and 10 are plotted with shaded error tubes to show variance. Similarly, the aggregated EMG analysis in Figure 11 utilizes bar plots with explicit error bars to quantify the statistical consistency of the changes.

> *(b) The autocorrelation analysis in Figure 6 should also include measures of lag if it's not at zero lag. If it's the latter, please specify it in the Methods.*

We thank the reviewer for this question regarding the cross-correlation analysis presented in Figure 6 (Panels G-J, P-Q). We confirm that this analysis was performed at zero time lag. To clarify this, we have added a sentence to the Methods section (Subsection "Crosscorrelation analysis") explicitly stating that the EMG cross-correlations shown in Figure 6 were calculated at zero lag. We have also added a clarifying note ("at zero time lag") to the description of these panels within the Figure 6 caption.

> *(c) Seeing EMG patterns similar to those presented in Figures 3D and 4D at different times post-lesion (e.g., as a Supplementary figure) would also give readers a better intuition of the neural changes.*

We thank the reviewer for this suggestion to provide more intuitive examples of the neural changes. We realize we did not sufficiently highlight this in the main text, but this complete data is already available in the manuscript. Supplementary Figures S1 and S2 provide a comprehensive overview of the EMG patterns for all recorded muscles in Monkey A and Monkey B, respectively. These figures show the pre-surgery and post-surgery average profiles for all recording sessions as well as the average profiles from five different post-surgery landmark days, covering the entire adaptation period. We have added explicit cross-references to these figures in the main text.

> *(d) I couldn't fully understand the analysis in Figure 4E; clarify.*

We thank the reviewer for noticing this oversight. The reviewer is correct that Figure 4E was not referenced in the main text. This panel was intended to show the baseline kinematic profiles (MCP and wrist angles) for Monkey B's control session, corresponding to the average EMGs shown in panel 4D. Given that our more comprehensive kinematic analyses are now presented in Figure 12 and the new Figure 13, we believe panel 4E is largely redundant. To improve the clarity and focus of Figure 4, we have removed panel 4E and its description from the revised manuscript.

> *(e) Some figures showing neural changes (e.g., Figures 6G-J, 6P,Q, Figures 9 and 10, and even Figure 11 for different reasons) would become more understandable if they were accompanied by the behavioural changes (e.g., something like Figure 5A on top of them).*

We agree that visualizing the temporal link between neural reorganization and behavioral recovery is essential for interpreting the data. We have implemented this suggestion by

overlaying behavioral metrics onto the right y-axes of Figures 6 (G-Q), 9, 10, and 11. However, regarding the specific behavioral metric, we opted to overlay the maladaptive behavior/aberrant reaching metric (from Figure 5B) rather than the grip formation time (Figure 5A). We found that the maladaptive behavior profile provided a clearer and more direct correlate to the neural data, as its peak coincides precisely with the 'swapped' synergy phase, thereby effectively illustrating the functional cost of that specific neural state.

> *(f) Some figure captions could be improved by adding more detail (e.g., for Figure 6).*

We agree. We have substantially expanded and improved the captions for Figure 6 and Figure 7 to make them more self-contained and guide the reader more effectively through the key findings presented in the panels. We have also reviewed other captions for clarity.

> *(g) I'd show the cosine distance between synergies across days as a main figure, e.g., as part of Figure 7, because this is an important result.*

We agree that the longitudinal stability of the synergy structures is a crucial result that deserves prominence. We have implemented this suggestion by adding a new panel, Figure 7 (I, K) for primary synergies and Figure 8 (K, L) for secondary synergies, which plots the cosine similarity of the spatial synergy weights across the entire experimental timeline. This figure explicitly visualizes the high stability of the pre-surgery baseline (blue traces, similarity > 0.99) and contrasts it with the dynamic structural tuning observed during the post-surgery adaptation (red traces), providing a clear, day-by-day account of synergy evolution as requested.

> *(h) In Figure 7C, D and G, H, it'd be interesting to also see in the background the EMG for the transferred muscle that belongs to each synergy, to appreciate their relationship.*

We thank the reviewer for this suggestion. To illustrate the close relationship between the primary synergies and their key constituent muscles, while avoiding visual clutter in the complex post-surgery plots, we have modified the pre-surgery panels of Figure 7 (C, D, G, H). In these panels, we have now overlaid the average pre-surgery EMG profile of the primary transferred muscle belonging to that synergy (e.g., FDS for Synergy A, EDC for Synergy B) as a thin, gray, dashed line. This visually confirms the tight correlation between the synergy profile and the muscle's activity at baseline.

> *(i) In page 10, the authors report as maladaptive behaviour the duration of the aberrant reaching component from day 29 (monkey A) and day 20 (monkey B). What was happening before those recording dates? Were the monkeys recovering?*

Thank you for this question. We have added two sentences to the start of the Results section ("Functional Recovery Follows...") clarifying that the period between surgery and formal recordings included approximately one week of home cage recovery followed by several weeks of assisted task practice. Formal recordings began once the monkeys could perform the task consistently without assistance.

> *(j) In the Methods (EMG Analysis), the authors state that they resumed their recordings post-TT "once they (the monkeys) were able to perform the task on their own". It would be good if the authors made this more precise (e.g., based on success rate or another metric).*

We thank the reviewer for this suggestion to increase precision. We have revised the Methods section to include the specific criteria used for resuming post-surgical recordings. Recordings were restarted once the monkeys were able to perform the task independently (i.e., without assistance from the experimenter) and consistently achieved a successful trial count of at least 100 trials within a single experimental session.

> *(k) Line 266- reads "Alternation of EMG activity in non-transferred muscle suggests one possibility: TT might alter the control strategy of coordinated muscle activity for hand movement by modifying the transferred muscles and their agonists as a cohesive unit", however, some "muscles showed patterns that were incompatible with a simple swap" (Lines 255-256). Doesn't this observation suggest that what happens is not a simple change in muscle synergies?*

We thank the reviewer for this insightful question regarding the interpretation of muscles with adaptive patterns incompatible with the primary 'swap-and-revert'. We agree that these observations require careful consideration within the modular framework. Our interpretation is that these muscles do not represent evidence against modular control, but rather reflect the involvement of multiple modules adapting concurrently. Specifically, muscles like FCR and PL, which showed distinct patterns, are primary members of Synergy C (the wrist flexor synergy) in Monkey A. Their adaptive profile is therefore consistent with the task-specific recruitment and retiming of Synergy C as part of the compensatory tenodesis strategy, rather than being a deviation from the swap observed in Synergies A and B. Synergies represent the dominant, shared variance in muscle activity. While they capture the overall strategy, some degree of individual muscle variation or the influence of secondary synergies is expected. We have added a sentence to the Results section to clarify that these diverse patterns likely reflect the differential involvement of muscles in multiple adapting synergies. We believe the overall evidence still strongly supports the modulation of stable synergies as the primary mechanism of adaptation in this paradigm.

> *(l) You may want to call synergy A and synergy B, synergy F and synergy E to make recall easier? (Same for synergy C and D, which could be F2 and E2).*

We thank the reviewer for this helpful suggestion aimed at improving clarity. We considered renaming the synergies based on function (e.g., F/E). However, given the number of figures and the complexity of a global change, and the fact that the functional roles of Synergies C and D differed between animals, we decided to retain the original A/B/C/D labels for consistency. To ensure clarity for the reader, we have carefully checked the manuscript to ensure that we consistently define the primary functional role of each synergy (e.g., "Synergy A, the primary finger flexor synergy") when it is discussed.

> *(m) Lines 315-317 - "These pattens of changes in synergy 3 and 4, both contributed minimally to the EMG of transferred muscles" -> This statement puts the causality as synergies cause muscles to activate according to certain patterns, which is supported by work by several groups -including the authors- however, they could also reflect biomechanical and task constraints as other have argued; perhaps this tone would be better for the discussion?*

We thank the reviewer for this nuanced point regarding the interpretation of synergy contributions. We agree that the causal relationship between computed synergies and muscle activity is complex and can reflect both neural commands and task constraints. To address this, we have revised the sentence in question in the Results section. Instead of stating that the synergies "contributed minimally," we now state that the changes in these synergies "were associated with minimal EMG activity in the transferred muscles." This phrasing is more descriptive of the observation and less implicitly causal, while retaining the key point within the flow of the results. The subsequent sentences, which offer interpretation, are already framed speculatively ("This suggests...", "may have served...").

> *(n) Line 403 How do the authors conclude from the synergy patterns in Figure 11 that the early post-TT is characterised by "an unstable and inefficient neural control strategy"? To me, this is shown clearly in the behaviour, not in these plots, unless I'm missing something?*

We thank the reviewer for this comment, which highlights the need to clearly connect our neural findings to the behavioral outcome. The reviewer is absolutely correct that the behavioral data (Fig. 5) provides the most direct evidence of instability and inefficiency during the early adaptation phase. Our intention was to argue that the neural patterns observed in Figure 11 provide a physiological correlate for this behavioral inefficiency. Specifically, the escalating aggregated EMG activity observed in the conflicted extensor synergy (Synergy B), which we term the 'arms race', represents significant muscle co-activation. Such co-activation is widely understood to be energetically costly and reflects a suboptimal control strategy where the CNS is essentially "fighting itself" against the altered mechanics. To make this link clearer, we have revised the concluding sentence of the relevant paragraph in the Discussion ("The early adaptation phase...") to explicitly state that this escalating co-activation is a known marker of inefficient recruitment and that it occurred concurrently with the period of poor behavioral performance shown in Figure 5.

> *(o) Lines 469-471. The authors suggest that muscle synergies may be preserved post-TT because a modular approach (to motor control) may be computationally easy and metabolically cheap. To me, recent data suggest that the most parsimonious explanation is what they later say: that the nervous system may not be plastic enough to change this (e.g., see Makin and Krakauer, "Against reorganisation" also in eLife).*

We thank the reviewer for raising this important theoretical point and for referencing the relevant literature on constraints on cortical reorganization. We agree that the preservation of muscle synergies in the face of such a profound perturbation is a key finding that warrants careful interpretation. In our revised Discussion (section "The CNS Defaults to a Modular Strategy..."), we have now explicitly incorporated the perspective that synergy stability may reflect inherent constraints on neural plasticity, citing Makin and Krakauer (2023), alongside our original hypothesis regarding computational and metabolic efficiency. We present these ideas not as mutually exclusive, but as potentially complementary factors that both contribute to the CNS's apparent preference for modulating existing modules rather than fundamentally restructuring them.

> *(p) Lines 501-503. Also on interpretation. Would the metabolic cost indeed be much higher? Couldn't the observed change in strategy be explained purely based on performance metrics?*

This is an important point. We agree that statements regarding high energy expenditure are interpretations, not direct measurements. We have carefully revised the manuscript (Abstract, Results, and Discussion) to soften these claims, using more speculative language (e.g., "likely costly," "what we propose was...") to clearly distinguish our interpretations from direct empirical findings.

> *(q) Lines 538-. The authors link the initial adaptation phase to the fast process reported in adaptation studies and say that this leads to poor retention. However, it seems from their data that the behaviour is stable across (early) days, so doesn't this rule out such an interpretation?*

We thank the reviewer for this insightful question regarding the interpretation of the early adaptive phase within the two-state model framework. The reviewer correctly notes that the early post-surgical behavior, while maladaptive, appeared relatively stable across days and did not show the rapid decay sometimes associated with the "poor retention" characteristic of the fast system. We agree that this apparent stability requires careful interpretation. In our revised Discussion (section "A Multi-Timescale Model..."), we now propose that the fast system is primarily responsible for the initial, rapid adoption of the 'swap' strategy in response to the large error signal. The subsequent persistence of this flawed but stable state for several weeks is likely not due to strong retention by the fast system itself, but rather reflects the time

required for the parallel slow system to gradually develop a more effective compensatory strategy (i.e., the tenodesis grasp). Once this alternative strategy became viable, it enabled the abrupt "switchback," which we also attribute to the fast system recalibrating away from the highly costly swap strategy. Therefore, we believe our data is consistent with the involvement of a fast system driving rapid strategic shifts, even if the typical "poor retention" phenotype is masked by the lack of a viable alternative strategy during the early phase.

> ***Reviewer #2 (Recommendations for the authors):***
>
> *(1) The discussion would benefit greatly from a more careful comparison with prior work characterizing the response to experimental or clinical tendon or nerve transfer in different models.*

We thank the reviewer for suggesting these important references and for the recommendation to compare our findings more carefully with prior work. This is an excellent point, and we agree it will significantly strengthen the discussion. In our full revision, we have added a new paragraph to the Discussion section dedicated to this comparison. We discuss how our findings relate to classic work showing primate adaptive capacity beyond simple maladaptive responses (Sperry, 1947), EMG evidence for the persistence of original neural patterns alongside new ones in human patients (Illert et al., 1986), the critical role of altered peripheral biomechanics and myofascial force transmission in complicating adaptation (Maas & Huijing, 2012), and how our observation of synergy stability aligns with evidence for modular adaptation strategies (Berger et al., 2013). This comparison helps situate our unique findings of a multi-timescale process and synergy timing modulation within the broader context of motor relearning after musculoskeletal rearrangement.

> *(2) Line 90 - Which disease or condition is studied in Hunter and Eckstein (2009)?*

Thank you. We have clarified this in the Introduction; the reference pertains to osteoarthritis.

> *(3) Line 280 for clarity in text and as a reminder to the readers, please state which muscles are involved in each synergy grouping.*

We have updated the text (Results, 'Adaptation occurs through modulating...') to explicitly list the main contributing muscles for each synergy grouping (e.g., Synergy A: FDS and FCU for Monkey A). This provides the requested clarity regarding the functional identity of each synergy while maintaining readability. For the complete, quantitative muscle weight composition including minor contributors, we referred the reader to Figure 7 and Supplementary Table 1.

> *(4) Line 180 There are differences in the time course for measurements between the behavioral metrics and EMGs. If not recorded at fixed time intervals, the differences in the time courses for the two monkeys should be explained.*

We thank the reviewer for this question regarding the time courses of our measurements. We interpret this comment in two ways, both of which we have addressed in the revised manuscript.

First, if the reviewer is asking about the overall recording schedule, they are correct that sessions were not performed at fixed daily intervals, and the specific days sampled differed between monkeys. This non-uniform sampling was due to the practical constraints of longterm behavioral experiments (e.g., animal cooperation, scheduling, weekends) and the aim to capture data during key phases of adaptation. However, within any given session, behavioral (video) and EMG data were always collected concurrently.

Second, if the reviewer is asking whether the set of days included differs between the behavioral plots (e.g., Fig 5) and the EMG/synergy plots (e.g., Figs 6, 9-11), this is a possibility depending on data quality criteria. Our criterion for including a session in the behavioral analysis was a minimum of 20 successful trials. However, for the more demanding synergy analysis, we required a higher minimum of 100 successful trials to ensure robust factorization. It is possible that a few sessions met the behavioral criterion but not the synergy criterion and were thus excluded from the latter analysis, leading to slight differences in the days presented across figures. To ensure full clarity, we have added text to the Methods section explicitly stating: (A) the rationale for the non-uniform daily sampling schedule, and (B) the specific minimum trial count criteria used for including data in the behavioral versus the synergy analyses, noting if this resulted in different sets of days being analyzed for different figures.

> *(5) General figure comments - The figures are informative, but they could be better presented, designed, and formatted to explain the important results in the paper. The figures should be able to explain most of the key results without entirely referring to the text to find some of the details. I had a bit of trouble understanding Figure 9 & 10. I would also like to suggest that bringing raw data into some figures (e.g., EMG of different muscle groups), such as showing stability between the synergies, could improve the results and allow the story to flow with more clarity. Likewise, clearly showing the differences between baseline EMG measurements and post-surgery measurements could improve some of the result figures.*

We thank the reviewer for these important general comments on data presentation. We agree that the figures are the key to our story and are implementing several revisions based on this and other reviewer feedback to improve their clarity.

General Presentation: We have conducted a thorough review of all figures to improve layout, consistency, and font legibility (addressing R3, 1 and the Reviewing Editor's comments). This includes adjusting the layouts of Figures 3, 4, and 6 for better alignment and clarity.

Figures 9 & 10 (Cross-correlation): The reviewer mentioned having trouble understanding these figures. In our revision, we have substantially rewritten the captions for Figures 9 and 10 to be much more descriptive. We explicitly walk the reader through how to interpret the plots (e.g., "The ‘swap’ is evidenced by the drop in self-correlation... and a concurrent rise in antagonist-correlation...").

Including "Raw Data" (EMG): We thank the reviewer for this suggestion to provide more intuitive examples of the neural changes. We realize we did not sufficiently highlight this in the main text, but this complete data is already available in the manuscript. Supplementary Figures S1 and S2 provide a comprehensive overview of the EMG patterns for all recorded muscles in Monkey A and Monkey B, respectively. These figures show the pre-surgery and post-surgery average profiles for all recording sessions as well as the average profiles from five different post-surgery landmark days, covering the entire adaptation period. These figures directly visualize the swap-and-revert pattern in the transferred muscles and their agonists (e.g., EDC, ED23), as well as the diverse and complex adaptations in other nontransferred muscles (e.g., FCR, PL), as requested. To make this clearer, we have added explicit cross-references to Supplementary Figures S1 and S2 within the main Results section to ensure readers are directed to this detailed data.

Showing Differences (Pre vs. Post): To "clearly show the differences between baseline... and post-surgery measurements," we implemented the point-by-point statistical comparison of pre- vs. final-day synergy profiles (as suggested in R1, 2b). This has resulted in a new Supplementary Figure visually highlighting the precise periods in the task where the final profiles still differ significantly from baseline (Fig. S9).

We believe these additions (new figures and improved captions) will make the results much clearer and more self-explanatory, as the reviewer suggested.

> *(6) Figure 1 A table with all the acronyms would help with identifying all the muscles and their respective synergies (supplemental), especially when describing the muscles in the result of the discussion section.*

This is an excellent suggestion. We have created a comprehensive table (Supplementary Table 1) listing all muscle abbreviations, full names, primary functional groups, and assigned synergies for both monkeys. We have added a reference to this table in the Figure 1 caption and the Methods section.

> *(7) Figure 2 - is this mainly from Monkey A? If so, it should be stated.*

We thank the reviewer for pointing out this omission. We have updated the caption for Figure 2 to clarify that the example data shown (ultrasound, trajectories, and quantitative plots) are from Monkey A.

> *(8) Figure 3 & Figure 4 seems unbalanced because of the descriptive need to explain Monkey B's tasks? The figure alignments could be better.*

We thank the reviewer for this comment on the visual presentation of Figures 3 and 4. The reviewer's observation that the figures appeared 'unbalanced' was correct. This was a direct consequence of two issues: (1) the different tasks required slightly different schematics (the "descriptive need" the reviewer mentioned), and (2) the original Figure 4 contained an additional kinematic panel (formerly 4E) that was unique to Monkey B, which broke the parallel structure with Figure 3.

To address this and significantly improve the alignment, we have now moved the unique kinematic panel (formerly 4E) to a new Supplementary Figure (Supplementary Figure S8). This change has allowed us to re-arrange the panels in Figures 3 and 4 so that they now follow the exact same order. We have also adjusted the layout to ensure that corresponding panels are of a consistent size. We agree that this creates a much better visual balance and makes the comparison between the two monkeys far more direct and clear, as the reviewer suggested.

> *(9) Figure 5. It seems like the animals can still perform the task post-surgery, but with high variability. Maybe emphasize the differences in variability between baseline and postsurgery?*

We thank the reviewer for this suggestion to emphasize the changes in variability. We have now quantified this using the Coefficient of Variation (CV) for key behavioral metrics across different phases (Pre-surgery, Early, Mid, Late post-surgery). The results confirm the reviewer's observation of high variability post-surgery, particularly in the early phase. For instance, Monkey A's grip formation time CV spiked dramatically (Pre: 47% vs Early: 133%), while Monkey B's remained high (Pre: 82% vs Early: 76%). Interestingly, while Monkey A's variability returned close to baseline levels in the late phase (Late: 55%), Monkey B's variability increased further (Late: 97%), suggesting persistent inconsistency despite functional recovery.

We also observed metric-specific changes. Monkey A's pull time became less variable than baseline later on (Pre: 65% vs Late: 43%), suggesting refinement of that action. Conversely, Monkey B's grasp aperture remained consistently low throughout (Pre: 26% vs Late: 19%), indicating relatively precise kinematic control was maintained or quickly regained. We have added a summary of these findings to the Results section to provide a more complete picture of how behavioral variability evolved relative to baseline during the adaptation process.

> *(10) Figure 6 quite a confusing figure. This figure needs to be better presented. The figure legends are hard to see for Monkey A vs Monkey B. At first, I thought Monkey B's figure legend also represented Monkey A. I would suggest reorganizing the figures for clarity and coherence.*

We agree that the original presentation of Figure 6 was dense and potentially confusing. We have completely reorganized the figure to improve clarity and coherence.

(1) Clear Separation: The figure is now structured with a strict separation between Monkey A (Left Panels, A-J) and Monkey B (Right Panels, K-Q), with prominent headers for each subject to prevent ambiguity.

(2) Improved Legends: We have redesigned the legends to be larger and placed them explicitly within their respective subject's section to ensure it is immediately clear which data they describe.

(3) Visual Consistency: We have standardized the color schemes and axis layouts across this and all other figures to reduce cognitive load and facilitate easier comparison between subjects.

> *(11) Figure 12 - This figure is incomplete without Monkey A's results. The videos in the supplemental sections seem clear enough for some kinematic analysis. The story could be more supported with more thorough measurements of the kinematics from both animals to show how they differ over time and by highlighting the two phases. As a minor note, it would be helpful to present the kinematic data together with a schematic of when during the task the data are drawn from, using the % task range scale, since that is the standard throughout the paper.*

We thank the reviewer for their suggestions regarding the kinematic analysis. We agree that a parallel kinematic analysis for Monkey A, similar to that in Figure 12, would be ideal. We did attempt this. Unfortunately, while the supplemental videos for Monkey A are sufficient for observing the overall movement trajectory, they are not suitable for the detailed joint angle analysis the reviewer suggests. The videos for Monkey A were recorded at an insufficient frame rate that did not allow to reliably extract the rapid joint angle positions of the wrist and fingers during the grasping movement. This is the reason why this detailed kinematic analysis was limited to Monkey B, for which we had high-speed video recorded at 240 fps, allowing for a robust analysis of these fast movements.

We have, however, expanded our kinematic analysis for Monkey B to show the refinement of the tenodesis strategy over the full time course (New Figure 13), which does help to highlight the different adaptive phases for that animal. We have also clarified in the manuscript (e.g., in the caption for Figure 12) that the lack of Monkey A data for this specific analysis was due to the lowresolution and low-frame-rate video available.

We agree that defining the precise timing of the kinematic snapshot relative to our normalized task range is critical for accurate interpretation. In response, we have added a new panel (Figure 12C) that explicitly maps the kinematic snapshot to our standardized task timeline. This schematic clarifies that the joint angle analysis captures the hand configuration during the pre-shaping phase, specifically at 83 ms prior to object contact (which corresponds to -0.02% of the normalized task range). This ensures the kinematic data can be directly interpreted within the same temporal context as the EMG and synergy results presented throughout the paper.

> ***Reviewer #3 (Recommendations for the authors):***

> *First and most major: I found many of the figures much too small and incredibly difficult to read. Possibly the most difficult was Figure 7, where I had to zoom in a great deal to read what muscles corresponded to which bars. I don't have specific suggestions here other than to make sure that figures are legible.*

We thank the reviewer for highlighting this important issue. We have comprehensively revised the figures to ensure they are legible at standard publication sizes. Specific improvements include:

(1) Figure 7: We have significantly increased the font size of the x-axis muscle labels and optimized the bar chart spacing to ensure the muscle identities are readable without excessive zooming.

(2) Global Updates: Across all figures, we have increased font sizes for axis labels and titles, removed unnecessary whitespace to maximize the data-to-ink ratio, and exported all final figures in high-resolution vector formats to ensure clarity.

> *Second and more minor: I liked the setup of the manuscript, where the authors explained the unique benefits of their experimental methods and the question they were going after ("When confronted with structural changes to the musculoskeletal system, does the CNS adapt by modulating existing synergies, or by shifting toward more fractionated control strategies?"). However, the evolution of the paper made the answer to this question seem very confusing to me as I read it. The results show that monkeys initially modulated existing synergies in phase 1, but then reverted to the original modulation. This, in addition to the way the question was set up initially, made me think the conclusion was going to be that the synergies themselves changed in the second phase, but this paradoxically was not the case--synergies were stable throughout. I was left confused for the back half of the results section, until the discussion on tenodesis and developing compensatory movement strategies. So the answer is that the monkey learns by modulating existing synergies, but using different strategies in different learning phases. I'm not entirely sure how to avoid this confusion, but I wonder if there's a way to foreshadow this finding earlier on.*

We thank the reviewer for this valuable feedback on the manuscript's narrative structure. We understand how the initial framing (modulation vs. fractionation) followed by the reversion of the initial modulation could lead to confusion before the compensatory strategy is fully introduced. To address this, we have made two key adjustments in the revised manuscript:

(1) In the Introduction, after posing the central question, we have added a sentence to subtly foreshadow that the adaptive process might be complex and multi-phasic, requiring analysis over extended timescales.

(2) In the Results section, at the transition point between describing the reversion of the primary synergy timings and introducing the compensatory tenodesis strategy, we have added a short paragraph to explicitly signal that the reversion was not the complete solution and that a distinct compensatory strategy emerged concurrently.

We believe these changes improve the narrative flow, provide better signposting for the reader, and mitigate the potential for confusion identified by the reviewer, making it clearer that the ultimate solution involved modulating existing synergies but via different strategies across distinct learning phases. We appreciate the reviewer's help in identifying this area for improvement.

https://doi.org/10.7554/eLife.108684.2.sa0